

Particle Collimation in Radiation  
Detectors and its Applications  
for Neutron Spectrometry

---

August 1972

---

日本原子力研究所

Japan Atomic Energy Research Institute

## JAERI レポート

この報告書は、日本原子力研究所で行なわれた研究および技術の成果を研究成果編集委員会の審査を経て、不定期に刊行しているものです。

### 研究成果編集委員会

委員長 山本賢三 (理事)

#### 委員

天野 恕 (製造部)	高田 稔 (研究炉管理部)
磯 康彦 (企画室)	塚田甲子男 (物理部)
大内 信平 (材料試験炉部)	鳥飼 欣一 (原子炉工学部)
小山内正夫 (動力試験炉部)	長崎 隆吉 (燃料工学部)
大西 寛 (原子炉化学部)	能沢 正雄 (動力炉開発管理室)
小幡 行雄 (物理部)	藤田 稔 (保健物理安全管理部)
桂木 学 (原子炉工学部)	堀田 寛 (高崎研・研究部)
柴田 長夫 (技術情報部)	

入手 (資料交換による)、複製などのお問い合わせは、日本原子力研究所技術情報部 (〒319-11 茨城県那珂郡東海村) あて、お申しこみください。なお、このほかに財団法人原子力弘済会情報サービス事業部 (茨城県那珂郡東海村日本原子力研究所内) で複写による実費頒布をおこなっております。

## JAERI Report

Published by the Japan Atomic Energy Research Institute

### Board of Editors

Kenzo YAMAMOTO (Chief Editor)

Hiroshi AMANO	Minoru FUJITA	Hiroshi HOTTA	Yasuhiko ISO
Satoru KATSURAGI	Ryukichi NAGASAKI	Masao NOZAWA	Yukio OBATA
Hiroshi ONISHI	Masao OSANAI	Shinpei OUCHI	Nagao SHIBATA
Minoru TAKADA	Kinichi TORIKAI	Kineo TSUKADA	

Inquiries about the availability of reports and their reproduction should be addressed to the Division of Technical Information, Japan Atomic Energy Research Institute, Tokai-mura, Nakagun, Ibaraki-ken, Japan.

---

編集兼発行 日本原子力研究所  
印刷 科学図書印刷株式会社

# Particle Collimation in Radiation Detectors and its Applications for Neutron Spectrometry

Mitsuru MIZUHO

Oarai Research Establishment  
Japan Atomic Energy Research Institute

Received January 25, 1972

## Abstract

Several types of gas recoil fast neutron spectrometers were constructed and their performances were investigated including newly developed methods for particle collimation.

A spectrometer of the intermediate-thickness radiator type with a multi-hole collimator was constructed. The spectrometer was composed of three methane-filled proportional counters (A, B and C) arranged end-to-end (tandem) with a common center wire (anode). Between counters A and B there is a collimator with many holes which work as a proton collimator. A summing problem constantly encountered in the conventional spectrometers of this type was perfectly removed by using anode pulses for the neutron energy. A fast coincidence between the pulses from the counters A and B reduced the chance coincidence by a factor of  $\sim 5$ .

A method of electronic collimation using the newly developed scheme with fast coincidence was introduced in the system of proportional counters. The collimation characteristic was investigated using an alpha source, then the method was applied to the neutron spectrometry with monochromatic neutrons of 0.6~1.5 MeV. A coincidence faster than 100 nsec was possible, resulting in more reduced chance coincidences.

An other method of electronic collimation was also developed with a rise-time discrimination in the conventional counter. The method utilizes the difference in rise-time of output pulses. The particles parallel to the anode alone could produce rapid-rise outputs. Therefore, an electronic collimation was possible by means of a rise-time analyzer. The collimating performance of the method was also examined with alpha particles, then the feasibility of a new scheme of the neutron spectrometer was indicated.

By one of the two foregoing methods of electronic collimation, the conventional collimator in a neutron spectrometer was eliminated: Removing a collimator means a considerable reduction in the background. Both methods, however, had still some defects concerning the background. These were removed by combining the two methods.

The rise-time discrimination in the gridded ionization chamber could also be used for particle collimation. The method was used for the angle measurement and proved to be a new type of neutron spectrometer with a thin radiator foil. It also improved the spectrum quality in the alpha spectrometry.

The rise-time discriminations in a gridded ionization chamber and in a proportional counter could be used for the particle (or neutron-gamma) discrimination. Examples of the discrimination by the author and others are given to demonstrate the effectiveness of the methods.

Previous spectrometers are also reviewed and classified to show the usefulness and originality of the present methods.

## 放射線検出器における粒子コリメーションと その中性子スペクトロメトリーへの応用

日本原子力研究所 大洗研究所

瑞穂 満

(1972年1月25日 受理)

### 要 旨

ガスリコイル型中性子スペクトロメーターにおいて必要な粒子コリメーションに関して新しい方法を開発し合計5つの方式の中性子スペクトロメーターを可能にした。主な内容は次のようである。

(1) 速いコインシデンスの可能な多孔コリメーター型スペクトロメーターの開発, (2) 速いコインシデンスによるエレクトロニックコリメーション法の開発とその応用, (3) 比例計数管におけるライズタイム弁別型エレクトロニックコリメーションの開発とその応用, (4) 方式(2)(3)の併用によるスペクトルの改善法, (5) グリッドチェンバーにおけるライズタイム弁別型エレクトロニックコリメーションとその応用, (6) 比例計数管, グリッドチェンバーにおける粒子弁別およびアルファスペクトル改善法。

## Contents

1. Introduction.....	1
1. 1 Review of the conventional neutron spectrometers .....	1
1. 2 Proton-recoil counters.....	2
1. 2. 1 Proton-recoil phenomena .....	2
1. 2. 2 Proton-recoil neutron spectrometer without (proton) collimation.....	5
1. 2. 3 Proton-recoil neutron spectrometer with particle collimation.....	8
2. Previous Methods for Particle Collimation in the Neutron Spectrometer.....	9
2. 1 Collimation by detecting proton recoils.....	9
2. 1. 1 Recoil telescope with collimation by the counter arrangement.....	9
2. 1. 2 Recoil telescope with a multi-hole collimator.....	10
2. 2 Collimation by detecting scattered neutrons.....	12
3. Present Methods for Particle Collimation and Their Application for the Neutron Spectrometry .....	13
3. 1 Recoil telescope with a multi-hole collimator.....	13
3. 1. 1 Introduction.....	13
3. 1. 2 Principle of the spectrometer.....	13
3. 1. 3 Construction of the spectrometer.....	15
3. 1. 4 Gas filling and purity.....	15
3. 1. 5 Electronics .....	16
3. 1. 6 Counter efficiency and line shape.....	16
3. 1. 7 Double scattering and chance coincidence.....	18
3. 1. 8 Measurements and results.....	18
3. 1. 9 Conclusion .....	21
3. 2 Electronic collimation with fast coincidence technique in proportional counters...	21
3. 2. 1 Introduction.....	21
3. 2. 2 Principle and apparatus .....	22
3. 2. 3 Results and discussions.....	23
3. 2. 4 Application to the neutron spectrometry.....	26
3. 2. 5 Conclusion .....	28
3. 3 Electronic collimation in a proportional counter by rise-time discrimination.....	28
3. 3. 1 Introduction.....	28
3. 3. 2 Principle of the method.....	28
3. 3. 3 Apparatus .....	29
3. 3. 4 Measurements and discussions .....	30
3. 3. 5 Application to the neutron spectrometry.....	33
3. 3. 6 Conclusion .....	36
3. 4 Combined method of the two foregoing methods.....	36
3. 4. 1 Introduction.....	36
3. 4. 2 Results and discussions.....	36
3. 5 Electronic collimation with rise-time discrimination in a gridded ionization chamber.....	38
3. 5. 1 Introduction.....	38
3. 5. 2 Principle of the method.....	39

3. 5. 3	Experimental apparatus .....	40
3. 5. 4	Measurements and discussions .....	40
3. 5. 5	Conclusion .....	41
4.	Other Applications of the Rise-Time Method.....	42
4. 1	Application to neutron-gamma discrimination in a proportional counter.....	42
4. 1. 1	Introduction.....	42
4. 1. 2	Results and discussions.....	42
4. 2	Application to particle discrimination in a gridded ionization chamber.....	43
4. 2. 1	Introduction.....	43
4. 2. 2	Applications .....	43
5.	General Conclusion .....	47
	Acknowledgements .....	47
	References .....	48

## 目 次

1. 緒 論	1
1. 1 中性子スペクトロメーターの概観	1
1. 2 陽子反跳計数管	2
1. 2. 1 陽子反跳現象	2
1. 2. 2 陽子コリメーションをしない型の中性子スペクトロメーター	5
1. 2. 3 陽子コリメーションを行なう型の中性子スペクトロメーター	8
2. 中性子スペクトロメーターにおける従来の粒子コリメーション法	9
2. 1 反跳陽子によるコリメーション	9
2. 1. 1 検出器の配置によりコリメーションを行なう反跳テレスコープ	9
2. 1. 2 多孔型のコリメーターを用いる反跳テレスコープ	10
2. 2 散乱中性子によるコリメーション	12
3. 新しい粒子コリメーション法と其中性子スペクトロメトリーへの応用	13
3. 1 多孔型のコリメーターを用いる反跳テレスコープ	13
3. 1. 1 はじめに	13
3. 1. 2 スペクトロメーターの原理	13
3. 1. 3 スペクトロメーターの構造	15
3. 1. 4 ガスの充填法と純度	15
3. 1. 5 電子回路	16
3. 1. 6 効率とスペクトルの形状	16
3. 1. 7 中性子の多重散乱と偶発計数	18
3. 1. 8 測定と結果	18
3. 1. 9 ま と め	21
3. 2 比例計数管における速いコインシデンスを応用した電子的コリメーション	21
3. 2. 1 はじめに	21
3. 2. 2 原理および装置	22
3. 2. 3 測定結果と検討	23
3. 2. 4 中性子スペクトロメトリーの応用	26
3. 2. 5 ま と め	28
3. 3 比例計数管における立上り時間弁別を応用した電子的コリメーション	28
3. 3. 1 はじめに	28
3. 3. 2 原 理	28
3. 3. 3 装 置	29
3. 3. 4 測定結果と検討	30
3. 3. 5 中性子スペクトロメトリーへの応用	33
3. 3. 6 ま と め	36
3. 4 前記2つの方法を併用した中性子スペクトロメーター	36
3. 4. 1 はじめに	36
3. 4. 2 測定結果と検討	36
3. 5 グリッド付イオンチェンバーにおける立上り時間弁別を応用した電子的コリメーション	38
3. 5. 1 はじめに	38
3. 5. 2 原 理	39
3. 5. 3 装 置	40
3. 5. 4 測定結果と検討	40
3. 5. 5 ま と め	41
4. 粒子コリメーション法の他への応用	42
4. 1 比例計数管における中性子-ガンマ線弁別への応用	42

4. 1. 1	はじめに .....	42
4. 1. 2	応用結果と検討 .....	42
4. 2	グリッド付イオンチェンバーにおける粒子弁別への応用.....	43
4. 2. 1	はじめに .....	43
4. 2. 2	応用 例 .....	43
5.	結 論.....	47
謝 辞	.....	47
文 献	.....	48



## 1. Introduction

### 1. 1 Review of the conventional neutron spectrometers

The fact that neutrons have no electric charge means a small probability of interaction between neutrons and matter. This makes difficult to detect neutrons or analyze neutron energy, and requires a special approach for the neutron measurements. Moreover, there are large differences in properties between fast and slow (or thermal) neutrons resulting in a quite different scheme in measuring principle.

Nearly all spectrometers reported for neutron energies from 0.1 to 20 MeV depend on the observation of one of the followings; proton recoils from n-p scattering, neutron flight time, or products from the  ${}^3\text{He}(n,p){}^3\text{H}$  or  ${}^6\text{Li}(n,\alpha){}^3\text{H}$  reaction.

Most required properties for a neutron spectrometer are high signal-to-background ratio, good energy resolution, and high efficiency over a wide range of neutron energies. Photographic emulsions and cloud chambers have good energy resolution and good background discrimination; however, these advantages are nullified by the tedious processes in a track measurement. All other methods also have their own disadvantages:  ${}^3\text{He}$  counters, for example, have an inherent background due to the  ${}^3\text{He}$  recoils which makes difficult the measurement of neutrons at above 1 MeV<sup>1)</sup>. The energy resolution of time-of-flight spectrometers is low above a few MeV because the flight time is too short to measure by the existing electronic system and moreover the gamma discrimination is inferior below a few hundreds keV<sup>2)</sup>. Proton-recoil telescopes have low efficiency particularly at low energies.

Early proton-recoil telescopes usually depended on the selective detection of recoils at angle  $\theta$  so that neutrons of energy  $E_n$  produced a discrete proton group of energy  $E_p = E_n \cos^2 \theta$ . The telescope reported by AMALUDI *et al.*<sup>3)</sup>, probably the first, has a "thin" hydrogenous radiator. Recoil protons from the radiator are collimated in a near zero-degree direction and pass through two or more proportional counters in tandem to produce coincidences. Proton energy is estimated from the thickness of an absorber inserted between the counters so that the proton range terminates in the final counter. Energy resolution in the scheme depends on the thickness of the final counter. Telescopes of this type have usually been used for the detection of monoenergetic neutrons<sup>4,5)</sup>, but have also been used as spectrometers<sup>6-8)</sup>. Improvements were made by several workers by modifying one or more counters in the telescope as follows; the  $dE/dx$  loss was measured in one of the counters to reduce the background<sup>9)</sup>, proton ranges were measured electronically<sup>10)</sup>, and the final counter was made very thick so that most of the recoil energy was dissipated in this counter; this energy was taken for the total energy.

MOZLEY and SHOEMAKER<sup>11)</sup> increased the efficiency by replacing a foil radiator with a "medium-thick" radiator, which worked also as a radiation detector. The proton energy was given by the sum of outputs from the two detectors (*i. e.* a radiator and the final detector).

Telescopes with a relatively "thick" radiator were also reported<sup>13-17)</sup>. In these telescopes, a radiator was sufficiently thick for the proton range. Two methods of proton collimation were adopted as described in chapter 2. A method of proton collimation by detecting scattered neutrons<sup>14,15)</sup> did not improve the efficiency though the other method by GILES<sup>16)</sup>, did. A more efficient method is to evaluate the neutron spectra from integral spectra of recoil protons. An

analytical method reported by Pool<sup>18)</sup> was used conveniently in the combination with digital computer techniques<sup>20,21)</sup>. A gamma contribution, however, remains not estimated; therefore a neutron-gamma discrimination is important in this type of spectrometers.

Comparing the "integral" type spectrometer with the "differential" one with a proton collimation, the former will be advantageous for a widely distributed spectrum, while the latter for the detailed observation of a narrow energy region giving direct information on the neutron spectrum.

The present studies deal with some proton recoil spectrometers. The proton recoil spectrometers thus will be discussed in the latter half of this chapter, to show where the present methods belong to.

Chapter 2. deals with the previous methods of proton collimation which is essential in the "differential" neutron spectrometers, and for which the present methods are original.

Chapter 3. describes the newly developed methods of particle collimation and their applications for neutron spectrometry.

Chapter 4. is concerned with other applications of the present method, which are closely connected with neutron spectrometry.

## 1. 2 Proton-recoil counters

### 1. 2. 1 Proton-recoil phenomena

Fast neutrons collide directly with nuclei when they pass through the matter since neutrons have no electric charge. The recoiling nuclei, charged particles, are easily detected with a conventional radiation detector such as a proportional counter. Hydrogen nuclei (protons) are most widely used as the recoiling nuclei in neutron detection and spectrometry; they are called "proton recoils".

In most cases, collisions of neutrons with light nuclei are elastic up to a few MeV, and can be treated nonrelativistically (Fig. 1). If a neutron of energy  $E_n$  in the laboratory system

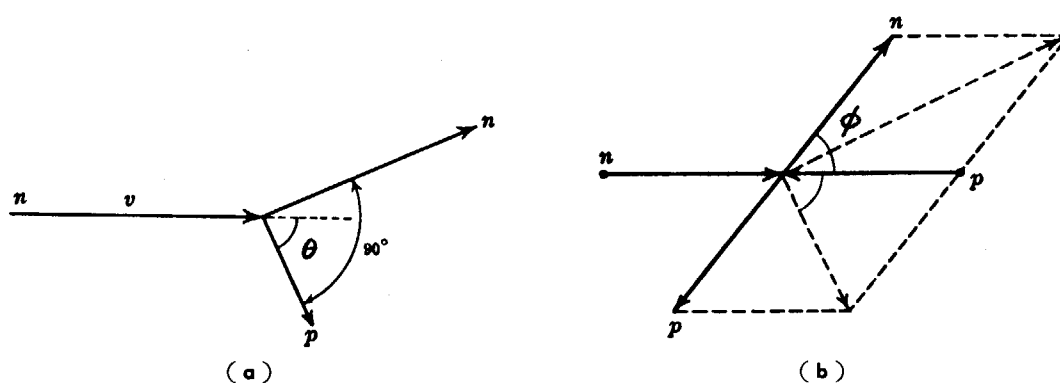


Fig. 1 Neutron-proton scattering as viewed, (a) in laboratory system and (b) in center-of-mass system.

collides with a nucleus of mass  $M$  originally at rest, the energy  $E$  of the recoil nucleus is calculated from the conservation law of energy and momentum. It is given for the recoiling particle with a recoil angle  $\theta$  as

$$E = E_n \frac{4M}{(M+1)^2} \cos^2 \theta. \quad (1)$$

If  $\sigma_c(\phi)$  is the differential cross section per unit solid angle in the center-of-mass system for the

elastic collision, the number  $dN_n$  of neutrons scattered between the angle  $\phi$  and  $\phi+d\phi$  by  $N_n$  incident neutrons is given by

$$dN_n = 2\pi N_n N_H \sigma_c(\phi) \sin \phi d\phi, \tag{2}$$

where  $N_H$  is the number of target nuclei per unit area, and  $\phi$  is the scattering angle of neutrons in the center-of-mass system. The same number of particles recoils in the opposite direction. Therefore, the equation (2) can be written for the recoiling particles  $dN$  between the angle  $\theta$  and  $\theta+d\theta$  in the laboratory system as

$$dN = 2\pi N_n N_H \sigma_c(\phi) \sin \phi \frac{d\phi}{d\theta} d\theta. \tag{3}$$

For an elastic collision in which target nucleus is originally at rest, the angle  $\theta$  and  $\phi$  are related by

$$\theta = \frac{\pi - \phi}{2}. \tag{4}$$

Combining the above relations together, the number  $dN$  of recoils with energies between  $E$  and  $E+dE$  in the laboratory system is given by

$$dN = N(E) dE = 4\pi N_n N_H \sigma_c(\phi) \frac{dE}{E_{\max}}. \tag{5}$$

$E_{\max}$  is the maximum energy of recoils, which correspond to the head-on collision ( $\theta=0$ ), and is given by

$$E_{\max} = \frac{4M}{(M+1)^2} E_n. \tag{6}$$

In the most frequent case of proton recoils, the equation (6) is simplified to  $E_{\max} = E_n$ .

The reasons why proton recoils are so commonly used for neutron measurements are: first, the recoil of protons by neutrons is isotropic in the center-of-mass system for a wide range of neutron energies up to  $\sim 10$  MeV; second, the energy of proton recoils is larger than for any other particle and is sufficiently large compared with that of carbon recoils; third, the cross sections are well studied and accurate within a few percent, and the cross section itself is rel-

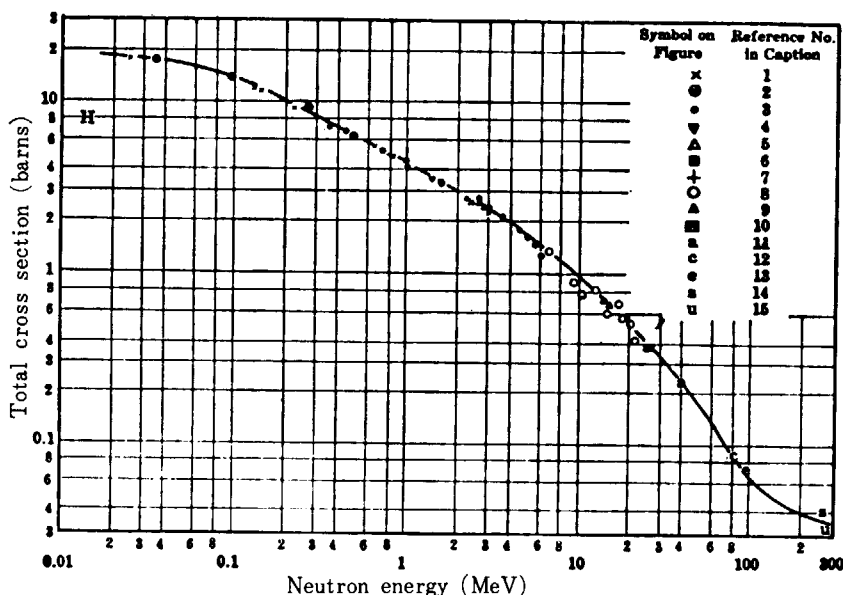


Fig. 2 Total neutron-proton cross section.  
 (by N. F. RAMSEY, in Experimental Nuclear Physics 1, E. SEGRE ed., John Willy & Sons Inc., New York, 1953)

atively large. (see Fig. 2)

If monoenergetic neutrons impinge on a hydrogeneous substance, the energy distribution of proton recoils is given by

$$N(E) = \frac{N_n N_H \sigma}{E_n}, \quad (E \leq E_n), \tag{7}$$

where  $\sigma$  is the total scattering cross section and  $\sigma = 4\pi\sigma_c(\phi)$ . The equation (7) shows that the proton recoils are distributed uniformly over the energy range of zero to  $E_n$  as shown in Figs. 3 and 4.

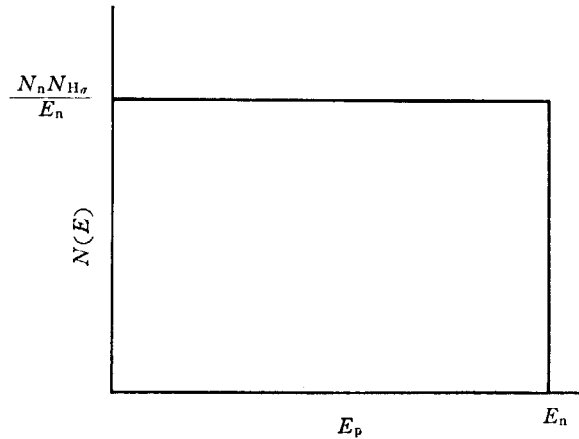


Fig. 3 Probability distribution of recoil energy  $E_p$ .

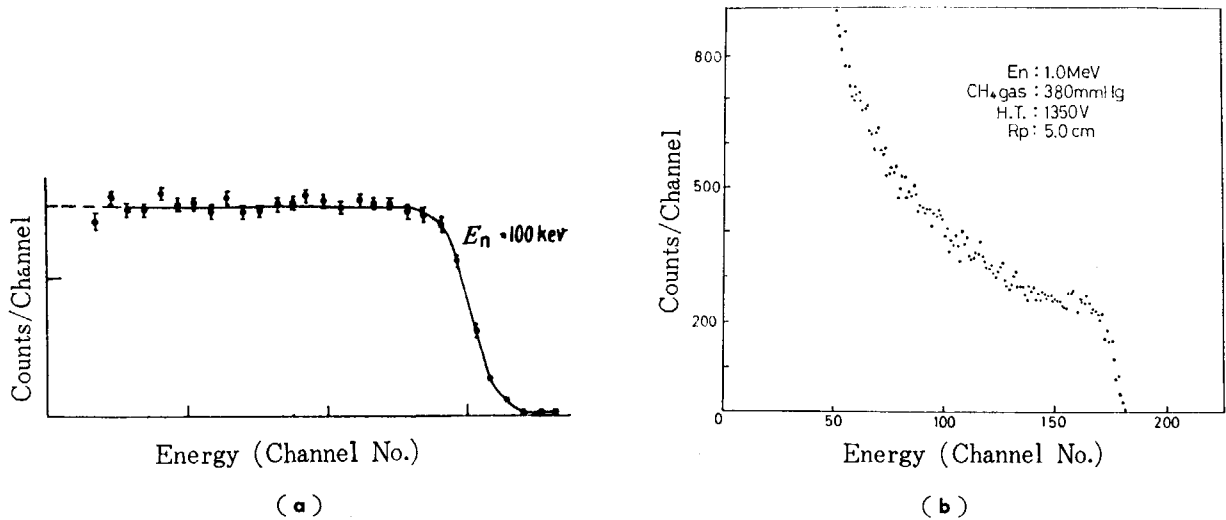


Fig. 4 Pulse-height distribution in proportional counters.

(a) Hydrogen-filled counter. Counter gas 130 cmHg, diameter of counter 5.0 cm, range of protons 0.2 cm ( $E_n = 100 \text{ keV}$ ). (by W. D. ALLEN *et al.*) (b) Methane-filled counter. Counter gas 38 cmHg, diameter of counter 6.2 cm, range of protons 5.0 cm ( $E_n = 1.0 \text{ MeV}$ ).

If neutrons are not monoenergetic, the energy distribution of proton recoils is given by

$$N(E) = N_H \int_E^\infty \sigma(E_n) N_n(E_n) \frac{dE_n}{E_n}, \tag{8}$$

where  $N_n(E_n)$  is the number of neutrons per unit energy interval at energy  $E_n$ . The equation (8) reveals that the incident neutron spectrum is evaluated from a energy spectrum of proton recoils by the relation

$$N_n(E_n) = - \frac{dN}{dE_n} \frac{E_n}{H_H \sigma(E_n)}, \tag{9}$$

This method is referred to the "integral" spectrum method in the present article.

A more direct method of determining the neutron energy is to observe only recoil protons scattered within a small solid angle in the forward direction  $\theta=0$ . In the case that neutrons are not monoenergetic, the energy spectrum is obtained after the efficiency correction, that is, multiplying the energy distribution of forward protons by  $1/\sigma(E_n)$ . This method is referred to the "differential" spectrum method in the present paper.

### 1. 2. 2 Proton-recoil neutron spectrometer without (proton) collimation

A proportional counter filled with a hydrogen-containing gas has been used in neutron flux measurements<sup>22)</sup> as a neutron "detector". However, the integral energy spectrum obtainable in this counter can be used for a mathematical evaluation of differential energy spectrum of incident neutrons. In early days, the evaluation was made analytically. However, the recent development in computer technique made possible the more accurate estimation of neutron spectra.

The main factors to be considered in this type of spectrometer are: a) elimination of the gamma pulses which are constantly observed in neutron measurements, b) distortion of the spectrum due to wall effect (only a part of the particle energy is measured for the tracks intercepting the detector wall), c) double or triple scattering of neutrons which makes the observed proton energy increased, d) recoiling nuclei other than hydrogen, such as carbon recoils which are familiar in the organic scintillator or in the hydrocarbon filled gas counter.

#### (1) Scintillation spectrometer by analytical evaluation

A technique for deriving neutron spectra from pulse-height spectra in an organic crystal was first proposed by POOL<sup>18)</sup>, and used to detect neutron groups from inelastic scattering of neutrons. Subsequently, a somewhat different method was developed by ELIOT *et al.*<sup>19)</sup> Both the methods required a separate experiment to remove the gamma contribution.

A method similar to Poole's, but with a gamma discrimination, was reported by BROEK *et al.*<sup>23)</sup> They derived a formula, taking into account the non-linear response of an organic scintillator; that is,

$$\frac{dN_n}{dE_n} = - \frac{E_n}{N_H \sigma} \left[ \frac{dL}{dE_p} \frac{d}{dL} \left( \frac{dL}{dE_p} \frac{dN_p}{dL} \right) \right]_{E_n=E_p} \quad (10)$$

where  $dN_p/dL$  is the number of protons per unit pulse-height interval.

The secondary scattering and wall effect were evaluated analytically; these events were subtracted from the undistorted spectrum, and spectra due to two factors were added to the reduced spectrum giving a spectrum with corrections (Fig. 5). Since the estimation of these factors is only approximate, it is desired to minimize these effects by choosing a crystal of suitable size.

#### (2) Scintillation spectrometer combined with a computer technique

In the spectrometers of this type, there are three problems to be solved; a) accurate determination of pulse-height distribution for monoenergetic neutrons, b) development of computer programs for determination of neutron spectrum from a measured pulse-height spectrum, and c) a neutron-gamma discrimination.

The pulse-height spectrum was usually determined by the use of Monte Carlo calculation; a report by BATCHELOR *et al.*<sup>24)</sup> for example. An improved method was reported by ZOLOTUKHIN *et al.*<sup>20)</sup>: a pulse-height spectrum due to single scattering was calculated "analytically" and other effects were with "Monte Carlo" method. The results are more accurate than those by the

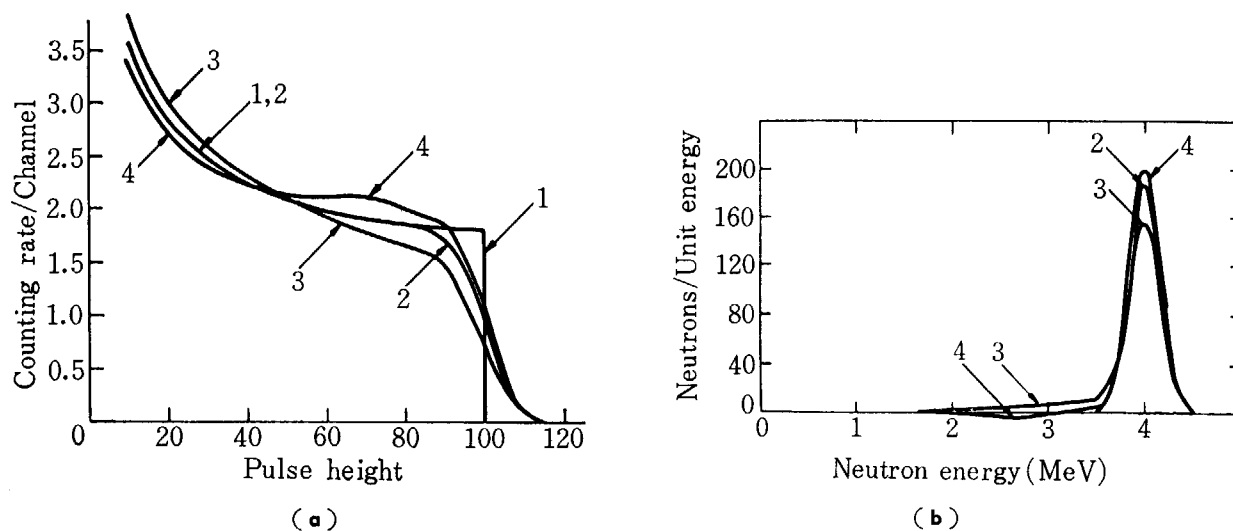


**Fig. 5** Calculated spectra produced in a stilbene crystal by monoenergetic 4 MeV neutrons (by H. W. BROEK *et al.*).

(a) pulse-height distribution. (b) deduced neutron spectrum.  
 Curves are; (1) perfect resolution, (2) 15% FWHM.  
 (3) wall effect for 1 mm thickness, (4) double scatter for 10 mm thickness.

conventional Monte Carlo method.

The evaluation of neutron spectra from the measured pulse-height spectra is quite tedious in an "analytical" method but easily accomplished with a digital computer. A "stripping method" which is essential for analysing a continuous neutron spectrum is reported by WASSON<sup>25, 26</sup> for example. A more efficient method is available for spectra consisting of one or more distinct neutron groups; that is, the integral method of SWARTS *et al.*<sup>27</sup>

### (3) Gas recoil counter

Gas recoil counter is suitable for the neutron spectrometer of this type: a) pure hydrogen gas can be used for a counter gas which means a high efficiency due to high hydrogen content and a freedom from carbon recoils, b) there is good linearity in the output pulse-height *vs.* absorbed energy, unlike the case in organic scintillators, c) neutrons with an extremely low energy (down to  $\sim 1$  keV) can be detected due to the low noise gas-multiplication in a proportional counter. Procedures to evaluate the neutron spectrum are similar to the scintillation spectrometers except the non-linearity correction which is unnecessary in the gas recoil spectrometers. These spectrometers, however, became practical with the newly developed methods of a neutron-gamma discrimination, which will be described independently.

Two examples were reported in this type of gas-recoil spectrometer. A cylindrical proportional counter filled with hydrogen or methane gas was successfully used by BENNET<sup>28</sup> as a neutron spectrometer. The spectrometer was used with a gamma discrimination, but without wall and multiple scattering corrections. He studied the  $1/E$  slowing-down neutron spectrum, and also the  $W$  function (the energy loss per ion pair). He pointed out that low-energy limitation of the spectrometer was rather firmly set about 1 keV by the increase in  $W$  at that energy and by statistics in the ionization and multiplication processes. An upper energy bound was estimated to depend upon confinement of the recoil proton to the counter proper, and if spherically symmetrical geometries are used to facilitate numerical treatment of distortion effects, one may obtain results at energies of 1 MeV, or perhaps somewhat higher.

BENJAMIN *et al.*<sup>29, 30</sup> used a spherical proportional counter filled with hydrogen gas. A more detailed calculation was adopted including wall and double scattering effects with a computer

code SPEC 4 and subroutines SPEC 28, SNIDOW and VSMTH. The code allows a complete analysis of an experimental recoil proton spectrum obtained. The only input data required in addition to the experimental spectrum are the counter parameters and an estimation of the neutron spectrum above the highest energy to be analyzed.

#### (4) Neutron-gamma discrimination

A gamma ray discrimination is unavoidable in this type of spectrometer, and is especially essential for low energy neutrons. Many authors<sup>31-47)</sup> have described the neutron-gamma discrimination in a scintillation spectrometer. The principal property used in these techniques is the difference in decay time of scintillation between different ionizing particles. It was first reported by WRIGHT<sup>31)</sup> between alpha particles and electrons in anthracene.

BROOKS<sup>32)</sup> and OWEN<sup>33)</sup> developed circuits to distinguish between heavily ionizing particles and electrons (gammas), which were sensitive to pulse-shape differences. BROOKS drew two signals from the last dynode and anode with different time-constants. They were summed to give zero pulse-height outputs for gammas, making it possible to distinguish against recoil protons which give outputs to certain extent. OWEN used a space charge limitation in an unusually connected photomultiplier. A relatively slow response was realized by a stage of weak electric field constructed with a special breeding. Such a photomultiplier responded differently to gammas (fast pulses) and to protons (slow pulses).

A zero-cross-pick-off (ZCPO)<sup>44-47)</sup> technique is also widely used to distinguish between the different decay times of gammas and recoil protons. Differentiating with a given time constant, differently decaying pulses give different zero cross points. The method could be used for a wide range of energy because a zero-cross point is not affected by the pulse height of outputs.

For a gas detector (proportional counter), BENNET developed a method of using a proportional counter in this field. Different specific ionizations *i. e.* different particle ranges in a counter gas, result in different rises of output. To emphasize the difference in particle ranges, a counter gas was filled up to the pressure where the range of protons was only 1~2 mm. A rise-time information was obtained by differentiating the output pulses with a delay line or with a fast stretcher<sup>48)</sup>. A modified Bennet method was developed by the authors<sup>49)</sup> and it will be described in chapter 4.

#### (5) Wall effect

An early attempt to eliminate the wall effect was to construct a "wall-less counter". A wall-less counter was used in a gas recoil neutron spectrometer by DOBROZEMSKY<sup>50)</sup>: the central counter is a proportional counter filled with hydrogen-containing gas, and is surrounded externally by 18 screening counters which are electronically connected in an anti-coincidence manner. The end-effect problem of realizing a sharp limitation at the both ends was solved with grids<sup>51)</sup> consisting of coiled helixes of 1.0 mm diameter and 1.1 mm pitch (7 windings of 100  $\mu$  wire). The uncertainty in delimiting the central volume in this arrangement amounts only to 0.1 mm in the axial direction. This arrangement is essentially insensitive to gammas which traverse a long range. With this "4 $\pi$ -anticoincidence" system and together with the "method of optimum pressure adjustment", it was possible to reduce the wall effect for neutrons of 50~300 keV.

For neutrons of a higher energy, it is convenient to use scintillation detectors. The optical problems in viewing a 4 $\pi$ -anticoincidence scintillators system may be solved by the method reported by the author<sup>52)</sup>: a central scintillator was surrounded by a second scintillator with different decay time, and both were seen with single photomultiplier. Only the particles dissi-

pating the whole energy in the first scintillator were recorded by the electric means, that is, decay time discrimination or pulse shape discrimination.

Recent attempts to correct for the wall effect include digital computer technique. In most papers dealing with a computer technique to calculate recoil proton spectra, the wall effect is also described. However, the most accurate treatment may be by SNIDOW<sup>53</sup>). He reported an accurate method of calculating the wall effect, in measuring an isotropic neutron flux with a spherical counter without a dead region and with a finite-length cylindrical counter with or without a dead region at each end. Analytical expressions are obtained for four path length probability functions, in which the geometrical aspects are handled in an exact manner. The path length probability functions and range data are applied to proton recoil spectrometers to determine the energy lost in the sensitive region by protons starting in either the dead region or the sensitive region and stopping in the gas or hitting the wall.

### 1. 2. 3 Proton-recoil neutron spectrometer with particle collimation

This type of neutron spectrometer has been most widely used since the earliest days of neutron spectrometry in spite of the rather low efficiency. The reason for this may be that definite information is obtainable on the energy spectrum.

The method of particle collimation is the most important in these spectrometers, and is a major subject dealt in the present paper. Therefore, more detailed description will be given in chapter 2.



## 2. Previous Methods for Particle Collimation in the Neutron Spectrometer

In this chapter, the conventional methods are classified according to the collimating scheme, to give general information how important the particle collimation is in neutron spectrometry. It is also shown what positions the present methods occupy in the types of the spectrometer.

### 2. 1 Collimation by detecting proton recoils

#### 2. 1. 1 Recoil telescope with collimation by the counter arrangement

##### (1) Recoil telescope with a "thin" radiator

COCHRAN *et al.*<sup>8)</sup> and JOHNSON *et al.*<sup>54)</sup> reported spectrometers of this type. A parallel beam of neutrons impinging on the radiator (a hydrogen-containing foil) produces proton recoils. Protons were detected or analyzed with a detector, which was a proportional counter in the Cochran spectrometer and a NaI (Tl) scintillator in the Johnson spectrometer; the detector was away from the radiator by an appropriate distance. The second or third counter, usually a proportional counter, was used to reduce background due to such as gammas and electrons. A proton collimation was realized by the geometry of radiator and detector. The distance between radiator and detector could not be reduced, and the diameters of radiator and detector could not be increased from the reason of energy resolution. The thickness of radiator was also limited to such an extent that the energy loss of protons in the radiator is not significant. These facts mean that only a low efficiency of the spectrometer can be achieved at a given energy resolution.

##### (2) Recoil telescope with a "medium-thick" radiator

These spectrometers were developed by MOZLEY *et al.*<sup>11)</sup> and CALVERT *et al.*<sup>12)</sup> and GELLER *et al.*<sup>55)</sup> to increase the spectrometer efficiency. The radiator in this type was organic scintillator; it was anthracene in Mozley's and Calvert's spectrometers and was stilbene in Geller's spectrometer. The output was taken from the radiator (the first crystal) and added to the output from the second crystal to give a total energy. These three spectrometers were used together with different types of second detector; it was anthracene in Mozley's and NaI in Calvert's, and a semiconductor counter in Geller's. The third detector, a proportional counter, is usually used between two detectors. A triple-coincidence among the detectors reduces the background. The proton collimation is achieved by the geometry of first and second detectors. The effective thickness of radiator depends on the neutron energy; it corresponds to the proton range at that thickness a minimum coincident output can be produced in the second detector. With a medium-thick radiator, the efficiency was increased by a factor of  $\sim 5$ , compared with the thin radiator type. The factor of only 5 was set by a lower hydrogen content in an organic crystal than that in a radiator foil. The category of "medium-thick" is by the present author, it belonged to "thick" by JOHNSON.

##### (3) Recoil telescope with "thick" radiator

This scheme of particle collimation slightly differs from that in the foregoing spectrometers. However, it was classified in a recoil telescope by JOHNSON.

In the scheme of collimation, protons lose a total energy in the radiator so that the radiator (detector) can be made sufficiently thick for the proton range. However, the counter diameter must be thin enough for protons with a recoil angle  $\theta \neq 0$ .

GILES<sup>16)</sup> constructed such a spectrometer: A main proportional counter with a transparent screen cathode was surrounded by 6 anticoincidence counters which occupied the space between the screen and outer cylinder tube. The whole traverse of proton recoils due to a beam of neutrons incident parallel to the counter axis remains within a main counter only for  $\theta \approx 0$ .

Protons intercepting the screen cathode ( $\theta \neq 0$ ) were not recorded as they were detected by one of anticoincidence counters.

BENENSON *et al.*<sup>17)</sup> analyzed the behavior of this collimating scheme. Main effort was directed to improve the peak-to-valley ratio of the instrument. For this purpose, end-effect counters were introduced at both ends, and the number of anticoincidence counters was increased to 12. A defect of this collimating scheme is that large angle recoils can not be rejected because of their short ranges due to small dissipated energies. These recoils make it impossible to measure neutrons of low energy with such pulse-heights.

However, this defect may be eliminated by the author's method<sup>57)</sup>: in this improvement, a main counter is divided into three or more counters by means of the divided cathodes or divided anodes method. A coincidence between these main counters removes large angle recoils since the recoils with a short range cannot produce simultaneous outputs among these counters.

The scheme of collimation may also be used with scintillation detectors: the spectrometer described by the author<sup>52)</sup> consists of thin cylindrical scintillators (the first detectors) and a surrounding (the second, anti-coincidence) scintillator with a different decay time. Recoils in the first scintillators are recorded if the range remains within the first scintillator. The spectrometer may be suitable for neutrons of higher energies and will have a higher efficiency than the gas spectrometer by a factor of the number of first scintillators.

### 2. 1. 2 Recoil telescope with a multihole collimator

The collimation in spectrometers described in the preceding section depends on the geometry of radiator and detector. A high efficiency in these spectrometers results in an alternative sacrifice in energy resolution. A high efficiency for a given resolution is possible only in the spectrometer with a multihole collimator, which is to be described in this section.

#### (1) Thin radiator spectrometer with a multihole collimator

This scheme of collimation seems not to be reported previously. The introduction of a collimator between radiator and detector will result in an increased background, so that it makes such a spectrometer impractical.

However, the rise-time method applied to a gridded ionization chamber, which is described in chapter 3, offers a new example in this category. The same collimating effects as a multihole collimator were realized electronically. The electronic collimation is free from the forementioned difficulty of background, making the method practical.

#### (2) Medium-thick radiator spectrometer with a multihole collimator

G. J. PERLOW<sup>58)</sup> used proportional counters in this scheme and studied the performance with monoenergetic neutrons. The pressure of methane gas chosen for a given neutron energy, and a region from 50 keV to 1 MeV was covered with this spectrometer. Two proportional counters were joined side by side. A multihole collimator, which was replaceable to provide a proper collimation for a required energy resolution, was placed between the two counters. Proton recoils

from  $\text{CH}_4$  in the first proportional counter are collimated and enter the second counter. The sum of pulses from the two counters is recorded whenever a coincidence occurs. A third counter, which follows the second counter, was connected in anticoincidence manner and discriminates against particles which do not lose all the energy in the first two. Efficiencies were calculated assuming a uniform beam with a cross-sectional area sufficiently large so that any collimator hole sees the same intensity of proton recoils as any other. Therefore, the efficiencies were calculated for any single hole taking into consideration the maximum acceptable recoil-angle, but not the effect of a collimator thickness.

Recently, a more accurate calculation was reported by LISKIEN *et al.*<sup>59)</sup> for a parallel beam and a point source. Calculations of open solid angle for a proton collimation, indispensable for the efficiency calculations, were performed without any neglect by a computer technique. The results of exact calculation were compared with those obtained with an approximation by CAPPELLANI *et al.*<sup>60)</sup> There were large differences especially for the small distances from the collimator (see Fig. 6).

For higher neutron energies, it is preferable to use scintillation detectors. Such a spectrometer appears not to have been reported yet except by the author.<sup>61)</sup> He tried to construct such a spectrometer using plastic scintillators with a low gamma sensitivity. As the demand increased for the spectrometry at lower neutron energies, a gas recoil spectrometer of this type was constructed. Details including the advantages and characteristics of the spectrometer will

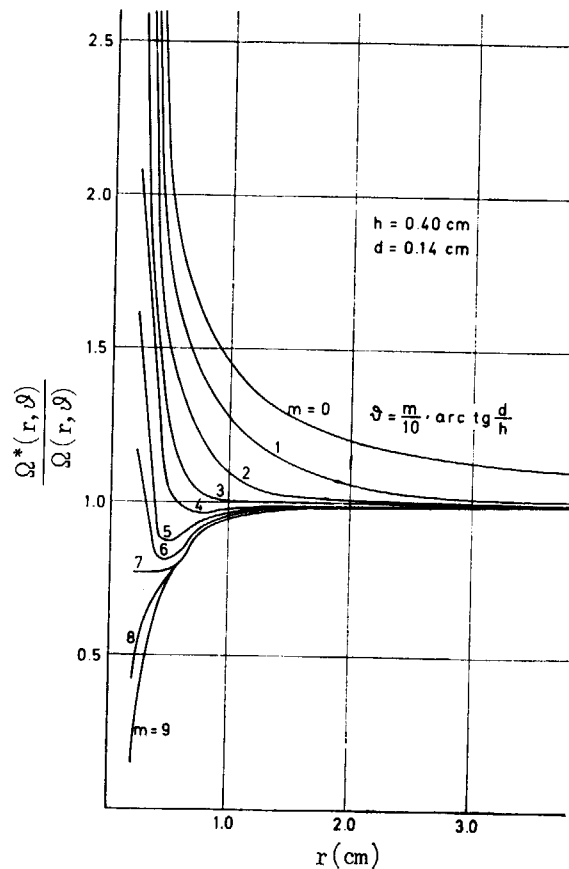


Fig. 6 Open solid angles  $\Omega^*$  obtained by an approximation compared with the exact ones  $\Omega$ . (by H. LISKIEN *et al.*) Notations are:  $r$  distance from a collimator hole to volume element where recoils start from,  $\theta$  angle viewing the volume element from a collimator hole,  $h$  thickness of the collimator plate,  $d$  diameter of the each collimator hole.

be described in chapter 3.

### (3) Thick radiator spectrometer with a multihole collimator

This type of spectrometer was impossible because protons could not be collimated in this spectrometer. However, a newly developed method for proton collimation described in chapter 3. enabled a spectrometer in this category. It is an electronic collimation by applying a rise-time discrimination in a proportional counter. A high efficiency is expected in this spectrometer, together with a low background and low gamma sensitivity.

## 2. 2 Collimation by detecting scattered neutrons

This scheme of collimation can be taken as a modification of the thick radiator type with proton collimation. The recoil angle of protons in a scintillation counter is defined by selecting the angle of scattered neutrons. An organic scintillator sufficiently thick for the proton range is illuminated by a beam of neutrons, and a second detector (a neutron detector) receives scattered neutrons from the first scintillator (a thick radiator). Proton signals in the first detector are recorded whenever they coincide with neutron pulses in the second detector. The collimation is defined by the geometry of two detectors.

Such spectrometers were reported by BEGHIAN *et al.*<sup>14)</sup> and DRAPER<sup>15)</sup>. In Beghian's spectrometer, the first detector (stilbene) was viewed by the second NaI crystal which was covered with silver plate and placed in a 90° direction. The second crystal detected gamma rays resulting from the capture of scattered neutrons (epithermal neutrons) by silver or iodine nuclei. Proton recoils, of which the corresponding scattered neutrons were detected at the second crystal, were registered giving an energy spectrum of head-on recoils.

In Draper's spectrometer, both crystals were stilbene; the second crystal detected fast neutrons instead of epithermal neutrons in the case of BEGHIAN *et al.*'s. The scattering angle was  $\pi/4$ : It is a compromise value since the product of resolution and efficiency is maximum at this angle for a given separation of the two detectors.

In these spectrometers, the second detector must be perfectly shielded against the incident and background neutrons and the background gammas to reduce background events. Practically, these spectrometers exhibited rather high background. Moreover, the efficiency was low since only a fraction of the neutrons scattered into the second detector was detected.

### 3. Present Methods for Particle Collimation and Their Application for the Neutron Spectrometry

#### 3. 1 Recoil telescope with a multihole collimator

##### 3. 1. 1 Introduction

A spectrometer consisted of two plastic scintillators and a multihole collimator, which was tried by the author<sup>61)</sup>, was expected to exhibit a high efficiency. It depends on the use of relatively large (compared with the distance between two detectors) scintillators, which became possible by the combination with a multihole collimator. Moreover, the gamma sensitivity could be reduced by the use of a semiconductor detector as the second detector. It is essentially insensitive to gammas and can be made as thin as just stop the proton recoils.

Recently, however, neutron spectrometry in the lower energy region has been required, which is mainly due to the demand from the fast breeder reactor. Therefore a gas recoil neutron spectrometer capable for keV neutrons was constructed<sup>62)</sup>. The improved spectrometer was designed to be suitable for the reactor experiment. It can be inserted into a beam-hole of reactors, so the shielding material can be reduced to a minimum amount.

##### 3. 1. 2 Principle of the spectrometer

###### (1) Principle

The spectrometer proposed here uses proton recoil phenomena caused by interaction of neutrons with counter gas in a proportional counter.

For the selection of recoil protons within the angle of  $\theta=0+\Delta\theta$ , the spectrometer is divided into three separate counters A, B and C, by means of divided cathodes and a common center wire. Between counters A and B there is a collimator disk for proton collimation (see Fig. 7). The negative signal from the common center wire is the main signal and corresponds to the proton energy  $E_p$ . On the other hand, outputs of counters A, B and C are taken from respective cathodes. The main signals from the center wire are fed to a gated multichannel pulse height analyzer (PHA). The gate is opened only when signals arrive simultaneously from

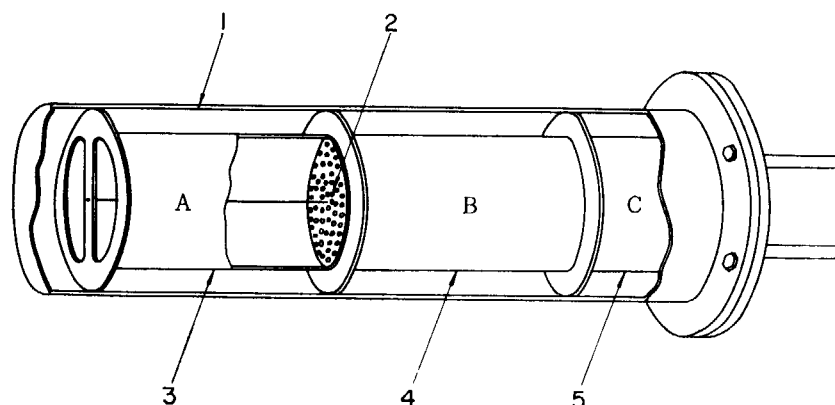


Fig. 7 Constructional sketch of the counter.  
Components are: (1) counter vessel, (2) collimator plate, (3)~(5) cathode cylinders of counters A~C.

counters A and B. Signals from counter C are used as anti-coincidence signal and close the gate of the PHA. Under such conditions proton recoils caused in counter A by neutrons entering parallel to the counter axis and having a recoil angle  $\sim 0^\circ$ , pass through the collimator and produce simultaneous (coincident) signals at counters A and B. By this procedure only the recoil protons with a recoil angle of  $\theta=0+\Delta\theta$  produce coincident signals in counters A and B and so the analyzed proton energies give the differential energy spectrum of the incident neutrons.

In the conventional spectrometers of medium radiator type, the proton energy  $E_p$  is given by summation of the outputs from counters A and B. In that case, the inequality between A and B coincidence counters and their circuits must be reduced as much as possible. In the counters the major source of inequality is the difference in diameters of the center wires. The required equality in the wire diameter was estimated by PERLOW<sup>58</sup>). In his case of 20 mil diameter the required equality was 0.1% ( $2 \times 10^{-5}$ ), because typically a 5% change in electric field changes the gas multiplication by a factor  $e$  ( $=2.718$ ). Of course, the gains of the two amplifiers can be trimmed to compensate for the inequality of the counters, but it is quite complicated because they must be re-trimmed whenever the operating condition such as voltage or gas pressure etc. is changed. To minimize the difference in diameter of the wires, it is recommended to use the successive lengths of a rod. In the present spectrometer,  $E_p$  is essentially given by the main signal from the center wire, and then it is possible to eliminate the summation circuit. This elimination has the advantage of unnecessary keeping the amplifier gains equal in the two channels and for matching the coupling capacitors or load resistors of proportional counters A and B.

The present spectrometer is also advantageous in the selection of the center wire. The use of a common center wire is evidently an advantage because we always use the successive lengths of a rod though the requirement of uniformity in the diameter still remains.

A disadvantage of this method to use the center wire pulses as the main signal is concerned with the pile-up. The pulse rate at the center wire channel is very high even when the coincidence rate of the counters A and B is low. A fast linear amplifier with good overload characteristics is preferable for the center wire channel. Also it is necessary to avoid the use of the spectrometer beyond such a counting rate that the pulse pile-up of the center wire channel is significant.

## (2) Possibility of faster coincidence

In general, fast coincidence is impossible with proportional counters. In the proportional counter the signal produced by the drift of primary ions is very small and practically the signal is produced by the secondary ions generated by the gas multiplication, which occurs in the small volume close to the center wire. The diameter of this volume surrounding the center wire is two or three times the diameter of the center wire.

The radiation incident upon the counter does not produce the signal immediately. Electrons of primary ionization are swept towards the center wire with a finite velocity and reach the multiplication region. At this time many ions are produced and an output signal is given. The time-lag between incidence of the radiation and the output is called "time jitter." This is generally of the order of  $\mu\text{sec}$  and depends upon the position of the primary ionization. A resolving time smaller than  $1 \mu\text{sec}$  is thus impossible for the coincidence with the proportional counter.

In the present counter, tracks to be measured are parallel to the center wire. This fact means a possibility of faster coincidence. Namely, there is of course a time jitter, but fortu-

nately two signals from counters A and B to be measured have the same time-lag because these tracks are equally distant from the center wire. A resolving time of 0.2 or 0.3  $\mu\text{sec}$  in the present case is determined not from the characteristic of the counter, but from electronics.

Reduction in the resolving time from the usual 1  $\mu\text{sec}$  to the present 0.2  $\mu\text{sec}$  means an important improvement with regard to chance coincidences. Generally, in the neutron spectrometer utilizing coincidence techniques, the chance coincidence rate is not small compared with the true coincidence rate, so it is very important to reduce the chance coincidences. A very simple estimation gives the reduction in chance coincidences to 0.2 ( $=0.2 \mu\text{sec}/1 \mu\text{sec}$ ).

### 3. 1. 3 Construction of the spectrometer

The spectrometer is essentially a proportional counter. Figure 7 shows the construction of the spectrometer schematically. The vessel for the counter gas has 120 mm *i.d.* and a length of 455 mm. Stainless steel was chosen to enable the use of a demountable metal gasket. A massive vessel is to be avoided since it increases the scattering of neutrons. The cathode cylinders of counters A and B are 0.15 mm thick, 90 mm in dia. and 150 mm long. The cathode of the anticoincidence counter C is shorter, only 70 mm long. A collimator for proton recoils made of 5 mm thick teflon plate with 800–1000 holes (2 mm dia.) is placed between counters A and B. Other supports for the cathode cylinders are also made of teflon. Though teflon was chosen due to the machinability, it is not the best for construction material as it contains hydrogen atoms which cause proton recoils and also fluorine which interacts with neutrons at higher energies. Both become possible sources of background. The requirements for collimator or supports are: (a) electrical insulation, (b) weak interaction with neutrons, (c) small desorption and adsorption of impurity gases, (d) easy machinability and (e) bakability. Ceramics *e.g.* alumina seems to be preferable with the exception of their machinability.

A nickel wire of 0.09 mm dia. was used as the center wire. To build up an electric field for a proportional counter, it is possible to apply either a positive high voltage to the center wire or a negative voltage to the cathodes.

For sealing of the vessel, a copper gasket was used. Hermetic seals for electric leads are welded using a minimum amount of soft solder and the inside is covered with "Araldite" to minimize the desorption. A valve with teflon gasket was provided for refilling of the counter gas, but it was replaced by a copper pipe seal-off after several tests.

### 3. 1. 4 Gas filling and purity

The baking is possible up to 250°C with a cooling of critical parts of the counter. This temperature may not be enough for baking, but a higher temperature requires to change the collimator material and soldering material for hermetic seals.

Methane was used as a counter gas. Prior to the gas filling, the counter was pumped and baked. The counter was pumped for a week to a high vacuum to supplement the insufficient baking temperature and care was taken not to expose the counter to the air. This procedure proved to be satisfactory. No special gas purifier was used for the following reasons: (a) the experiments were preliminary, and recoils of the other atoms than hydrogen were not of interest in this stage; (b) the energy resolution of the spectrometer was determined mainly by collimator opening; (c) the spectrometer gave a resolution of  $\sim 4\%$  for the  $^{210}\text{Po}$  alphas (see Fig. 12) and this is sufficient for a neutron spectrometer. An alcohol and dry-ice trap for moisture was used. Typical gas contents were:  $\text{CH}_4$  97.6%,  $\text{O}_2$  0.6%,  $\text{N}_2$  0.2% and  $\text{CO}_2$  1.6%.

### 3. 1. 5 Electronics

The electronic block diagram of the spectrometer is shown in Fig. 8. The coincidence circuit is used at 0.2  $\mu$ sec resolving time. It generates gate pulses by the arrival of negative

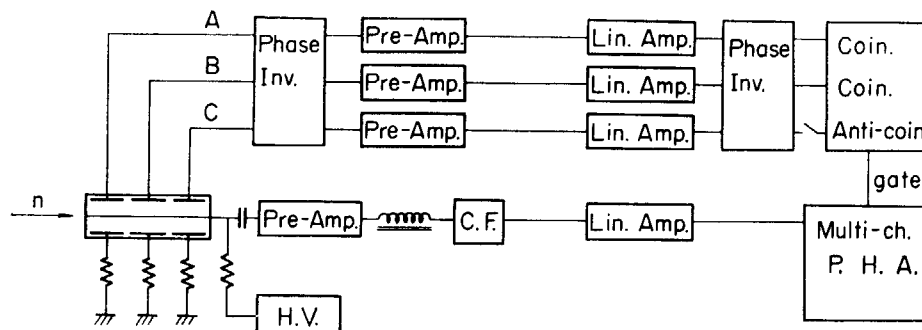


Fig. 8 Block diagram of the spectrometer.

input pulses of 2 V or more. Gain controls of the linear amplifiers in the coincidence and anti-coincidence channels were used to vary the effective discrimination level for coincidence pulses. The linear amplifiers were in the operating room, 30 m from the target room of the 2 MeV Van de Graaff accelerator. A faster coincidence than 0.2  $\mu$ sec cannot be used in the present system. For the faster coincidence, it is necessary to use a technique of "fast coincidence for slow pulses". A possible method is to add a derivative pulse to the original pulse. The derivative pulse is equal to the original one in profile but inverted in polarity and reduced in pulse height by a certain fraction. Two pulses are added together, such that the derivative is in advance of the original by  $t_r$ , where  $t_r$  is the rise-time of the original pulse. A zero cross pick-off technique is applied to the superimposed pulse. Any point in the leading slope of the original pulse can be selected as a timing point in this method by selecting the pulse-height fraction of the derivative pulse. Thus, faster coincidence for slow pulses becomes possible.

Delay of 0.47  $\mu$ sec (HH 1500 of 1.8 m) was necessary in the main signal line for the timing between the input and gate signals of PHA. Voltage sensitive pre-amplifiers were used in the spectrometer. Therefore it was necessary to minimize the length of the cables between counters and pre-amplifiers to avoid increase of input capacitances of the pre-amplifiers. If current-sensitive preamplifiers are used, it is possible to place them in the operating room because the connection of long cables up to about 100 m is possible.

### 3. 1. 6 Counter efficiency and line shape

It is most preferable to use the spectrometer for a parallel beam of neutrons though it is also to be used for a point source just as in the present case. For this reason the counter efficiency is calculated for a parallel beam. Considering the efficiency for a parallel beam it is convenient to deal with unit area of the counter.

The counter efficiency  $\varepsilon$  is defined as the ratio of counting rate per unit area of the counter to the neutron flux. A calculation was carried out according to Perlow's procedure<sup>58)</sup>; he gives the counter efficiency as

$$\varepsilon = \pi^{-1} \eta (a/d^2) n R_0 \sigma, \quad (11)$$

where

$\eta$  = transparency of the collimator at  $\theta = 0$ ,

$a$  = area of a collimating hole,

$d$  = thickness of the collimator,



$n$ =number of hydrogen atoms per unit volume at 15°C, 1 atm,  
 $R_0$ =range of protons in the gas at 15°C, 1 atm,  
 $\sigma$ =cross section of n-p scattering.

The present case of  $\eta \sim 0.40$ ,  $a = \pi \text{mm}^2$ , and  $d = 5 \text{mm}$ , results in

$$\epsilon = 0.17 \times 10^{-5} R_0 \sigma. \tag{12}$$

Results of the calculation using  $R_0$  from WHALING<sup>63)</sup> and  $\sigma$  from BNL-325<sup>64)</sup> are shown by the broken line in Fig. 9. But this calculation needs some correction for the present spectrometer, because in the spectrometer a theoretical consideration indicates that the isolation between counters A and B is not so good. An experimental result is shown in Fig. 10. A collimated beam of X-rays from <sup>55</sup>Fe is injected into the counter perpendicular to the counter axis

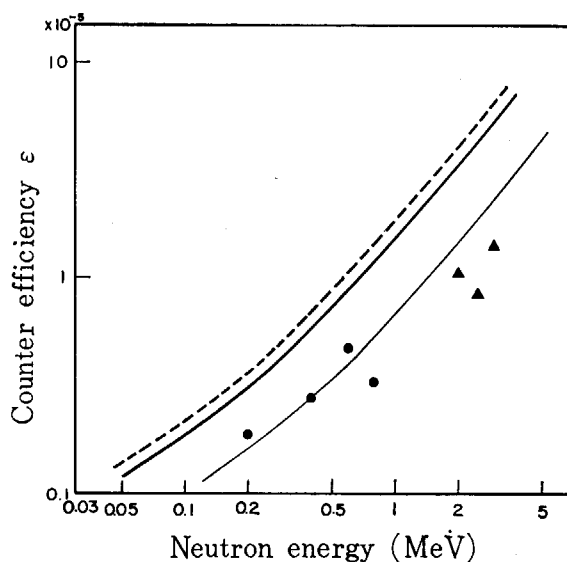


**Fig. 9** Counter efficiency vs. neutron energy.  
 Curves are: broken line; theoretical maximum without dead zone, thick solid line; theoretical maximum with 1.4 cm dead zone at 10 cm range, thin solid line; with 6 cm dead zone at 10 cm range.

through a thin aluminum window. From this result the trouble of self-coincidence is evident if the smallest signals of counters A and B are accepted without any discrimination. This trouble sets up a dead zone at both sides of the collimator. The thickness of this dead zone in counter A is estimated as 1.4 cm from Fig. 10.

The efficiency curve including dead zone effect is given by the solid line in Fig. 9 for a proton range of 10 cm. This gives the theoretical maximum of the efficiency for a proton range

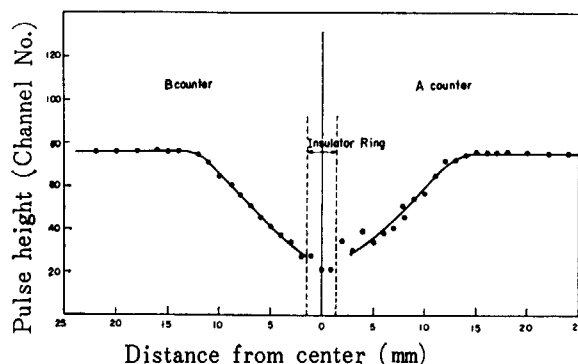


**Fig. 10** Isolating property between counters A and B (divided cathodes method).

of 10 cm, and practically it cannot be realized because it is rather difficult to set the discrimination level just to such a point.

In the measurements the discrimination level was so determined to reject self-coincidence with an alpha source on the collimator. But it was over-discrimination as shown in the measured efficiencies of Fig. 9. The dead volumes in these measurements were estimated to be 6 cm thick.

More accurate calculation of the counter efficiency and line profile are necessary for the precise measurements or to check the capability of the spectrometer for absolute measurements. The effect of the collimator thickness on the transparency of protons is neglected in this calculation though it is not so small. Recently LISKIEN *et al.*<sup>59)</sup> reported more refined calculations without this neglect.

### 3. 1. 7 Double scattering and chance coincidence

False coincidence from double scattering of neutrons, namely a neutron scattered by a proton in counters A or B causing again proton recoil in counters B or A, cannot be avoided essentially. The probability of double scattering increases at higher neutron energies.

Chance coincidence is caused from the finite resolving time of the coincidence circuit. Faster coincidence results in a smaller probability of the chance coincidence. In the present case of resolving time of 0.2  $\mu$ sec, it is reduced down to  $\sim 20\%$  of the ordinary value.

### 3. 1. 8 Measurements and results

Equation (11) shows that the efficiency  $\epsilon$  is independent of gas pressure, due to the approximations in calculation. In practice, acceptable  $\Delta\theta$  is large for recoils occurring near the collimator. Then a longer proton range due to a lower gas pressure results in a higher energy resolution and a lower efficiency. A longer range over 15 cm (length of counter B), however, is not preferable because it lowers the efficiency by the end effect. Anti-coincidence counter C was provided to suppress the background from an energetic particle like cosmic rays or electric noise which is apt to appear in counters A, B and C simultaneously, rather than as a rear end effect counter. Where a rear end effect counter is needed, the front end effect counter is also required to the same degree.

A shorter range is neither preferable: a proton range shorter than the previously-mentioned dead volume is meaningless and longer range is preferable from this point of view.

The separation of counters A and B is achieved by divided cathode cylinders. The discrimination levels were determined using an alpha source, they were 20% of the maximum pulse height to avoid the self-coincidences at 10cm ranges. These levels and ranges were maintained throughout most of the experiments.

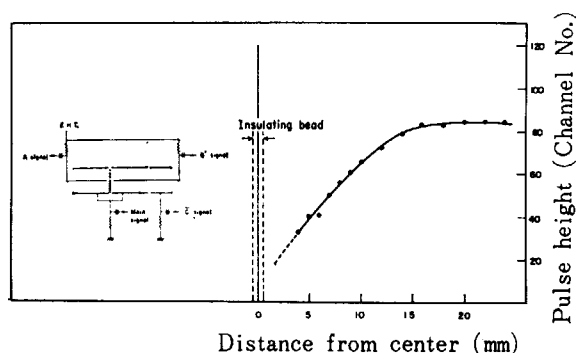


Fig. 11 Isolating property between counters A and B (divided anodes method).

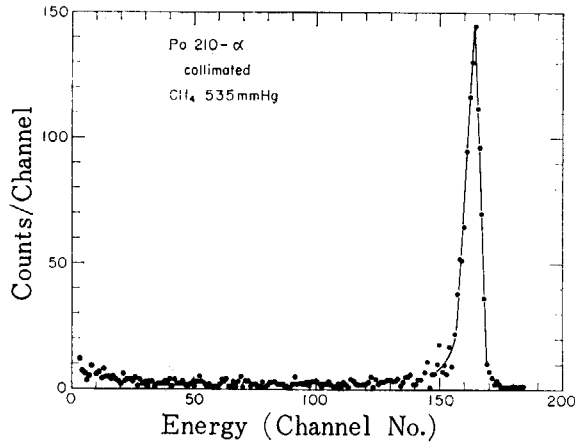


Fig. 12 Response of the counter for collimated alphas. Counter was operated as a conventional proportional counter.

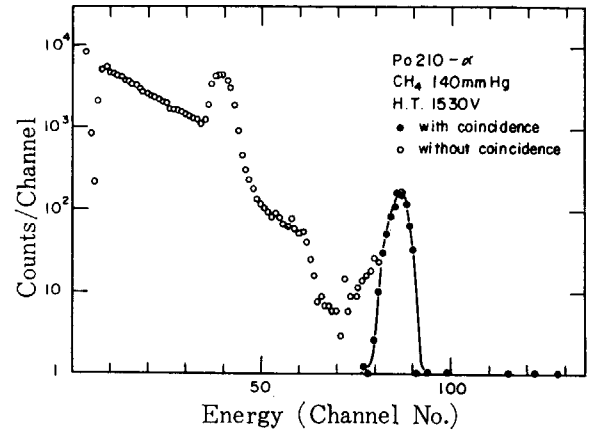


Fig. 13 Response of the spectrometer for alphas with and without coincidence.

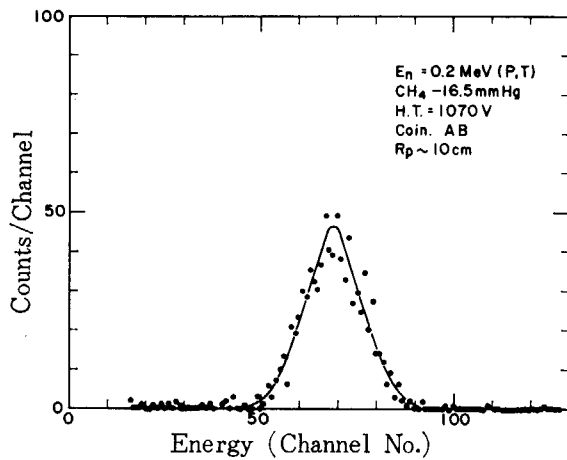


Fig. 14 (a) Response of the spectrometer for 0.2 MeV neutrons.

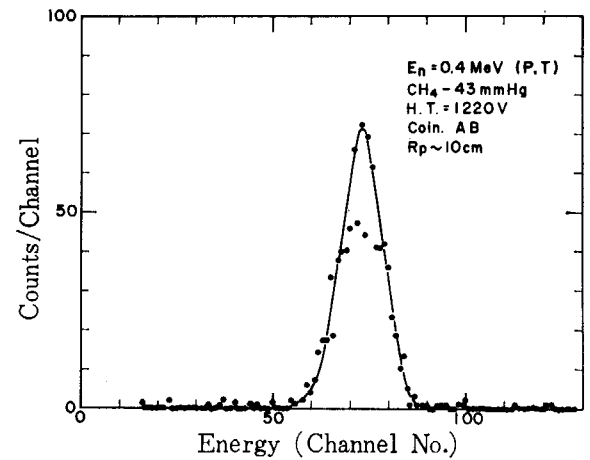


Fig. 14 (b) Response of the spectrometer for 0.4 MeV neutrons.

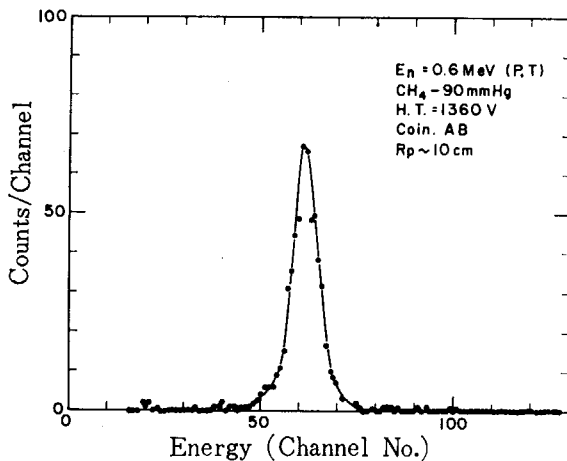


Fig. 14 (c) Response of the spectrometer for 0.6 MeV neutrons.

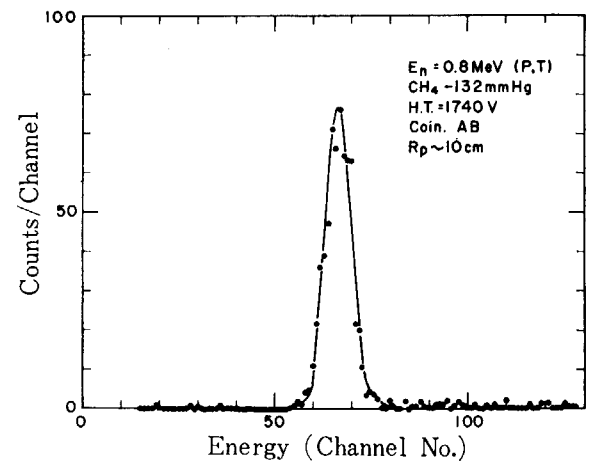


Fig. 14 (d) Response of the spectrometer for 0.8 MeV neutrons.

A method for avoiding the decrease in efficiency due to the A and B interaction is to use the collimator of semi-conductive material which acts as electrical shield between counters A and B without field perturbation, though such a collimator is rather difficult to realize. An attempt to minimize the interaction by use of divided center wires for separation of counters A and B does not lead to good results (see Fig. 11).

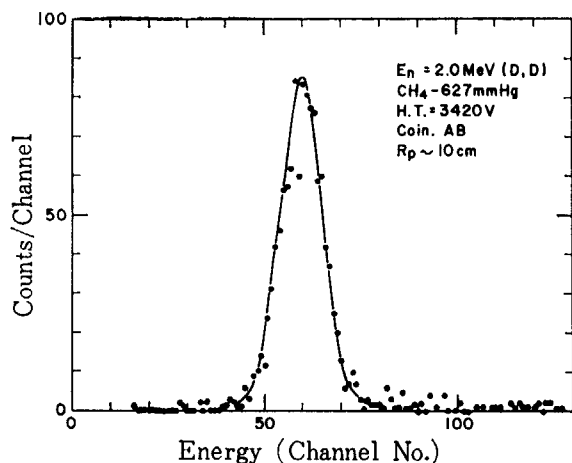


Fig. 14 (e) Response of the spectrometer for 2.0 MeV neutrons.

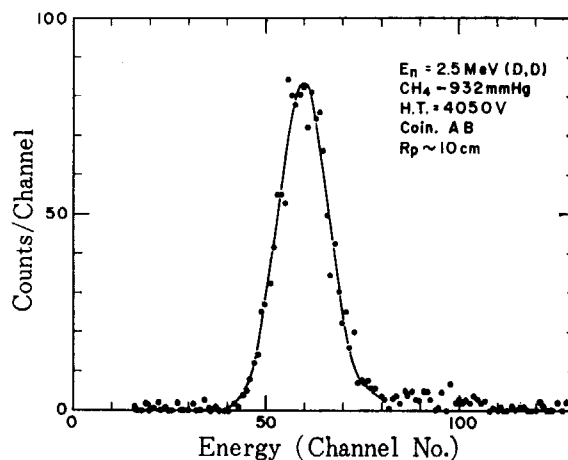


Fig. 14 (f) Response of the spectrometer for 2.5 MeV neutrons.

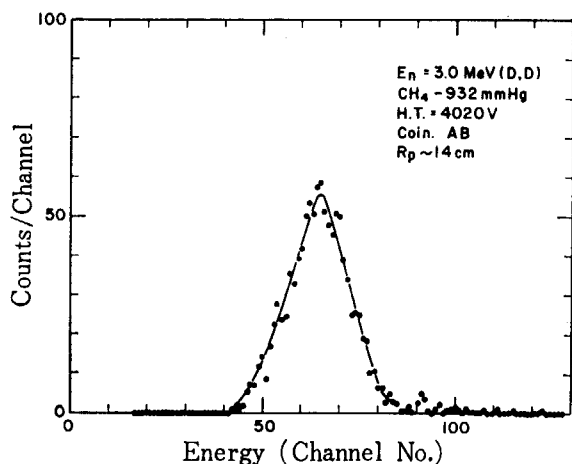


Fig. 15 Response of the spectrometer for 3.0 MeV neutrons.

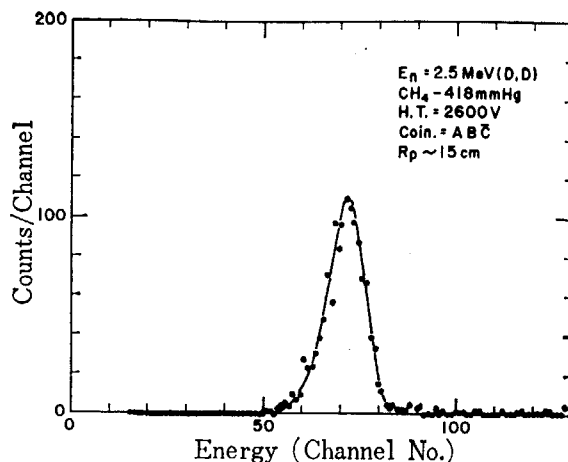


Fig. 16 Response of the spectrometer for 2.5 MeV neutrons at 15 cm range.

By applying a negative high voltage to the cathodes, a smaller influence of ripple or noise can be expected, but in the spectrometer positive high voltage was applied to the center wire to minimize the number of coupling capacitors of high working voltage. Ripple and noise are eliminated to a negligible level by adding an LC filter.

Measurements were made using a collimator with 2 mm dia. holes. Figures 12 and 13 show alpha ray tests. In Fig. 13 a peak due to alpha particles impinging on the collimator is observed around fortieth channel. Figures 14-16 are for neutrons. In Figs. 14 a-d, pulse-height spectra are shown for (p-t) neutrons of 0.2, 0.4, 0.6 and 0.8 MeV, respectively. In those cases the counter is placed in the forward ( $0^\circ$ ) direction. Figures 14e-15 are for (d-d) neutrons of 2.0, 2.5 and 3.0 MeV which were obtained at  $130^\circ$ ,  $100^\circ$  and  $80^\circ$  directions, respectively. Figures 15-17 are for longer proton ranges; here in the cases referred as  $ABC\bar{C}$ , counter C acts as the rear end effect counter. In Fig. 9, the observed efficiencies are indicated.

In the cases of (d-d) neutrons the incident neutrons are not monochromatic because the counter views the target at high angle of  $80^\circ$ - $130^\circ$  and stands with a large solid angle against the target. Energy spectrum of the neutrons incident on the counter was calculated for 3 MeV neutrons. An analytical estimation seemed to be difficult, and so the following method was adopted: By dividing the counter into parts with an angular interval of  $5^\circ$  and considering the geometrical weight, a histogram was obtained. The result is shown in Fig. 18. In the figure the energy spread of the incident neutrons was estimated to be  $\sim 7\%$ .

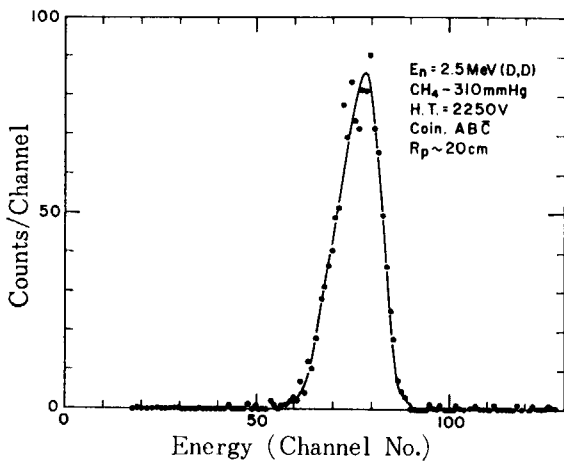


Fig. 17 Response of the spectrometer for 2.5 MeV neutrons at 20 cm range.

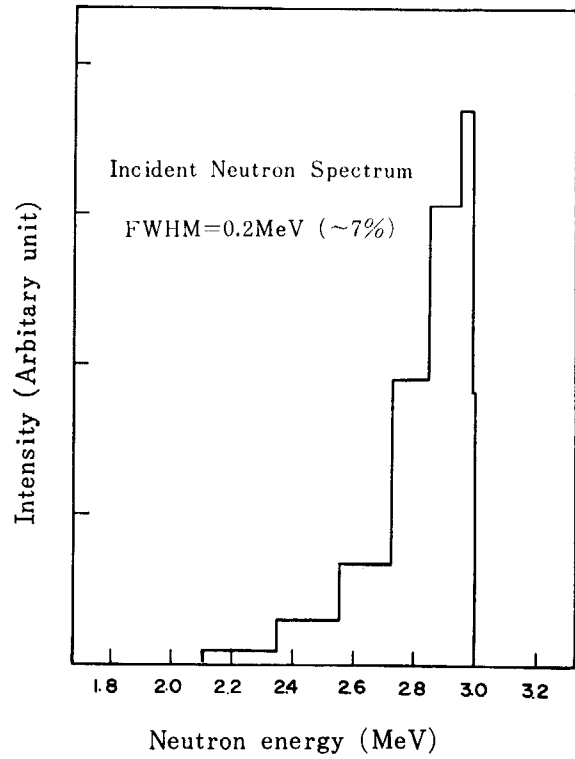


Fig. 18 Energy spectrum of incident neutrons.

### 3. 1. 9 Conclusion

An energy resolution of  $\sim 13\%$  was obtained for 0.6 and 0.8 MeV neutrons. For lower and higher energies the resolutions becomes inferior. For (d-d) neutrons there is a energy spread of incident neutrons resulting from the finite solid angle with which the spectrometer was seen by the target.

The observed efficiencies are lower than the theoretical values because of the over-discrimination (see Fig. 9). But there were many error-sources in the calculation of the efficiency : (a) neutrons were not in a parallel beam ; (b) simple volume correction for the dead volume was insufficient for the reason shown in section 3. 1. 8 ; (c) estimation of the discrimination level had considerable uncertainty, etc.

A poor consistency among the observed efficiencies is mainly caused by reason (c). Thus, to use this spectrometer for absolute measurement, more accurate calculations of the counting efficiency (including a line profile) and a method for accurate estimation of the discrimination level are necessary.

Observed counting efficiencies for 10 cm, 15 cm and 20 cm of proton range are consistent with the theoretical expectation (*i. e.*,  $\epsilon$  for 10 cm as well as for 20 cm are less than  $\epsilon$  for 15 cm). It is shown among Figs. 14 f, 16 and 17 ; these were obtained with the same counting time.

## 3. 2 Electronic collimation with fast coincidence technique in proportional counters<sup>67)85)</sup>

### 3. 2. 1 Introduction

In a previous section of this chapter, characteristics of the medium-thick radiator neutron spectrometer were reported. In section 3. 1. 2, it was pointed out that fast coincidence is pos-

sible between counters A and B on account of its particular geometrical arrangement. As a general rule, a value of around  $1 \mu\text{sec}$  is recommended for the coincidence resolving time with proportional counters<sup>5(6)</sup>, and faster coincidence has hitherto been considered impracticable because of time jitter in the proportional counter. The reduction in resolving time for coincidence permitted by the present approach is therefore an important improvement in neutron spectrometry for the reduction of background thereby made possible.

In the previous study, the resolving time attained of  $0.2 \mu\text{sec}$  was dictated not by counter performance but by the relevant electronics. Recently faster electronics has been constructed which has a capability of coincidence down to  $5 \text{nsec}$ . Such rapid coincidence between counters A and B has introduced the possibility—from theoretical consideration—of dispensing with a collimator. This is in turn an important advance in respect of background reduction, of increasing spectrometer efficiency, and of extending the possibilities in the choice of counter material and construction.

### 3. 2. 2 Principle and apparatus

#### (1) Principle of electronic collimation

Charged particles in the counter can be divided into three categories as shown in Fig. 19.

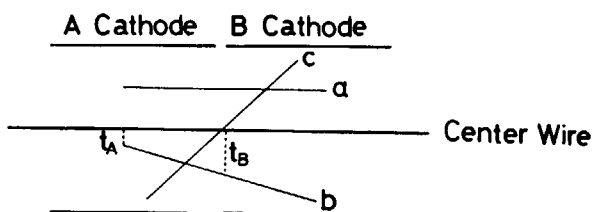


Fig. 19 Principle of electronic collimation (fast coincidence method).

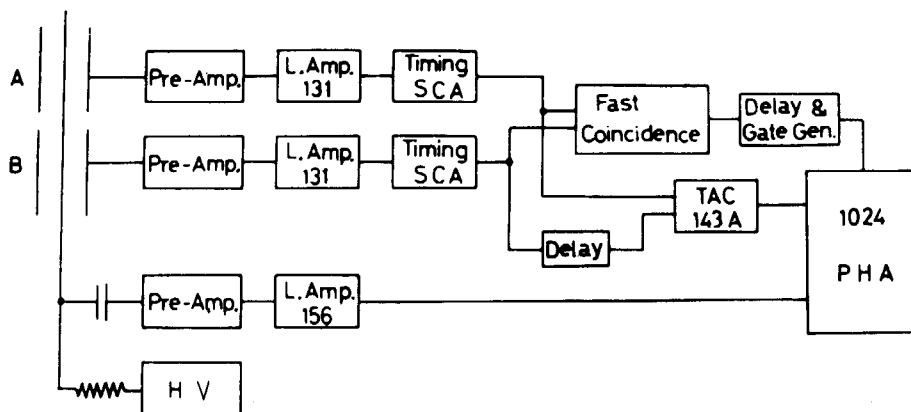


Fig. 20 Block diagram of measuring apparatus (fast coincidence method).

They are; (a) tracks are parallel to the center wire ( $t_A = t_B$ ), (b) not parallel to the center wire ( $t_A \neq t_B$ ), and (c) as a special case, not parallel but  $t_A = t_B$ , where  $t_A$  and  $t_B$  correspond to the time lags between the incidence of a particle and the output signals in counters A and B. The probability of the case (c) would be small (and particularly so for recoil protons caused by the parallel beam of neutrons) and therefore can be ignored at the present stage. By means of fast coincidence the  $t_A = t_B$  particles alone, *i. e.*, those incident parallel to the counter axis, can be selected with the use of a system such as shown in Fig. 20.

#### (2) Counter

The proportional counters system is arranged in a counter vessel made of aluminum (A-

1 B). The center wire (see Fig. 19) is stainless steel of 0.05 mm diameter. The cathodes of the counters A and B are also made of aluminum, 62 mm in innerdiameter and 130 mm long. They are arranged end-to-end along the same axis and are separated by a gap of 1 mm. In some cases it will be necessary to insert the third cathode between the two to keep apart the cathodes A and B each other without field perturbation and which will produce no signals. This is necessary in the case where interaction between counters A and B<sup>62)</sup> is not negligible. The above arrangement was chosen in preference to the divided center wire, based on the experience of previous experiments<sup>62)</sup>. Methane was used as counter gas in the present study. Water vapor in the gas was removed with a Mg(ClO<sub>4</sub>)<sub>2</sub> trap.

The electronic system is represented by the block diagram in Fig. 20. Signals from the counters A and B are amplified through the pre-amplifiers (double emitter follower) and JAERI (Japan Atomic Energy Research Institute) model 131 multi-mode amplifiers. This model 131 was used with either double delay line (DDL) shaping or double differentiation and single integration (RC) shaping to produce bipolar outputs. The shaping constant is 0.7  $\mu$ sec for the DDL mode and 2 $\mu$ sec-2 $\mu$ sec-2 $\mu$ sec for RC shaping. Canberra Industries model 1435 timing single channel analyzers (SCA) are used as the pulse height discriminator and zero cross pick-off (ZCPO) unit. They are equipped with variable delays for fine adjustment of the time lag between the signals A and B. The resolving time of the fast coincidence unit (Canberra Ind. model 1441) can be varied continuously from 5 to 100 nsec. The outputs of the SCAs are also fed to the time-to-amplitude converter (TAC) (JAERI model 143 A) to analyze the time distribution of signals B in reference to signals A. In this channel, the signals B are delayed by an appropriate amount using a variable delay (JAERI model 148) to ensure that signals A are always in advance of signals B. The energy signals are obtained from the center wire. The linear amplifier of this channel is a JAERI model 156 spectroscopy amplifier with variable active filters. A shaping time constant of 0.8  $\mu$ sec was used in this channel.

### 3. 2. 3 Results and Discussions

Measurements were carried out using alpha particles from an <sup>241</sup>Am source. The counter was used with 1 atm. of methane (flowing gas) with an applied voltage of 2,200 V. Under these conditions the gas multiplication was estimated to be 25, and the same conditions were maintained throughout the experiments.

**Photographs 1 (a)** and **(b)** represent two-dimensional dots-on-film display of energy (abscissa) vs. time distribution (ordinate). For this experiment, energy signals from the center wire were fed to the F side ADC (analog-to-digital converter) of a Nuclear Data 160 F multi-channel pulse height analyzer, and the outputs of the TAC (time-to-amplitude converter) to the M side ADC. The correlation between the two signals is displayed in the form of spots on a cathode ray tube via a digital gate (Nuclear Data 160 DG), used in high resolution (1,024  $\times$  1,024) mode. **Photograph 1 (a)** shows the uncollimated alphas and **Photo. 1 (b)** the collimated results obtained with DDL (double delay line) pulse shaping, while **Photos. 2 (a)** and **(b)** represent those with RC shaping. The dots representing the highest energy and smallest time delay are from particles incident parallel to the counter axis. Some particles are observed with a very small time delay and exceptionally low energy; these are alphas colliding the cathode. The lower energies observed in **Photos. 1 (b)** and **2 (b)** as compared to the corresponding uncollimated results is due to the energy loss in the collimator.

**Figures 21 (a)** and **(b)** show the time distribution of the signals B in reference to signals A for the collimated particles with different directions of incidence. The three lines represent collimated ( $2\theta=30^\circ$ ) particles of which directions are; (1) inclined by  $10^\circ$  with respect to the

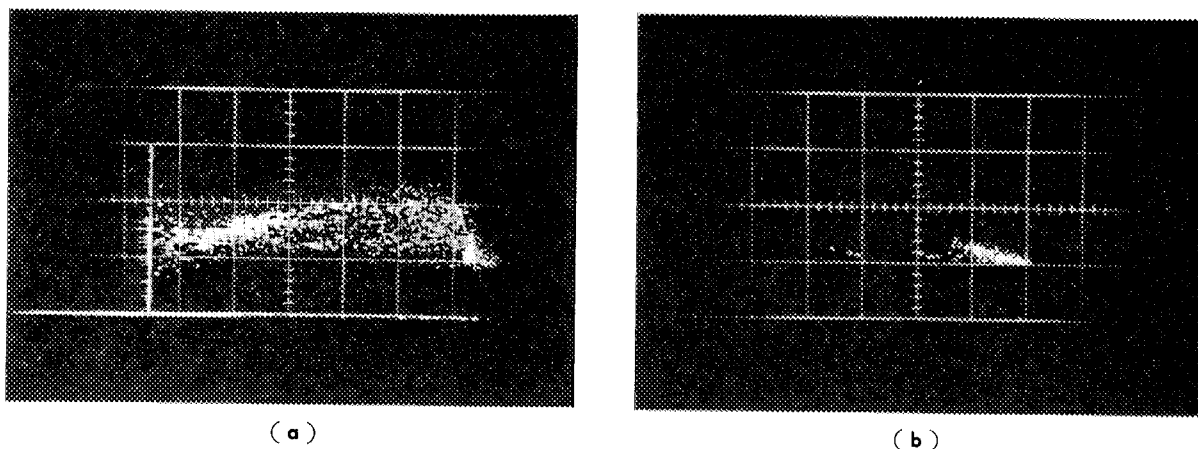


**Photo. 1** Two-dimensional display of energy (abscissa) *vs.* time-distribution (ordinate) in coincidence method. Pulse shaping ; DDL, source ;  $^{241}\text{Am}$ , counter gas ;  $\text{CH}_4$ -760 mmHg. Applied voltage ; 2200V. Scales ; abscissa 0.9 MeV/div., ordinate 200  $\mu\text{sec}/\text{div.}$ .  
 (a) Without collimator.  
 (b) Particles collimated ( $2\theta=40^\circ$ ) parallel to the center wire.

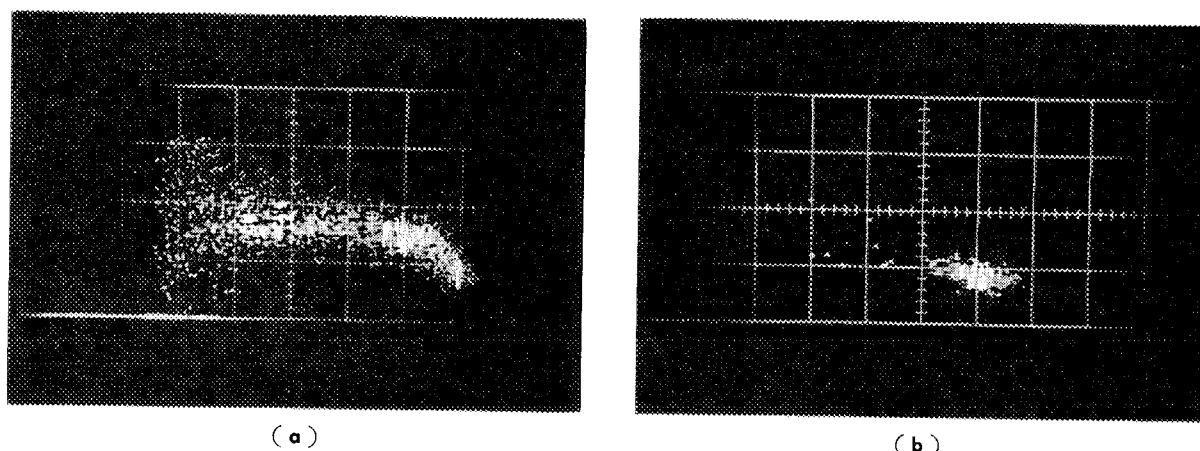


**Photo. 2** Two-dimensional display of energy (abscissa) *vs.* time-distribution (ordinate). Conditions are the same as shown in **Photo. 1** but RC shaping.  
 (a) Without collimator.  
 (b) Particles collimated ( $2\theta=40^\circ$ ) parallel to the center wire.

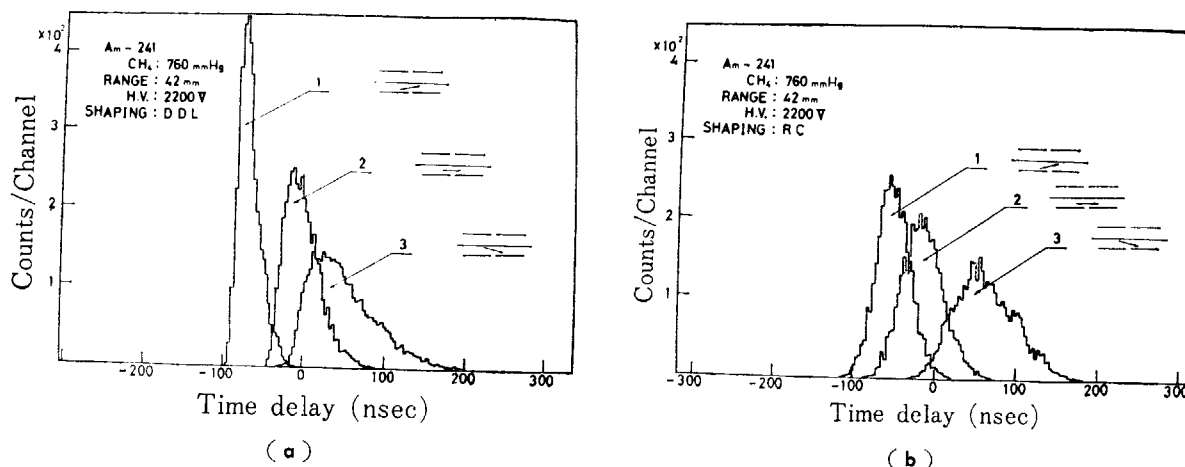


**Fig. 21** Time-distribution for alpha particles with different directions. Particles are collimated to  $2\theta=30^\circ$ , and directions are ; (1)  $10^\circ$  against the center wire, approaching to, (2) parallel to the center wire, (3)  $10^\circ$  against the wire, parting from.  
 (a) DDL pulse shaping. (b) RC pulse shaping.



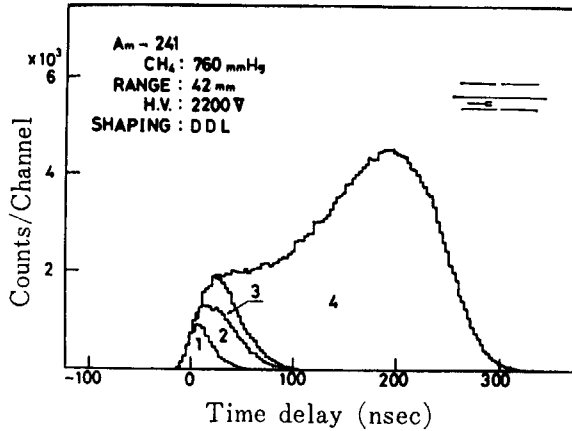


Fig. 22 Time-distribution with and without collimator (DDL pulse shaping).

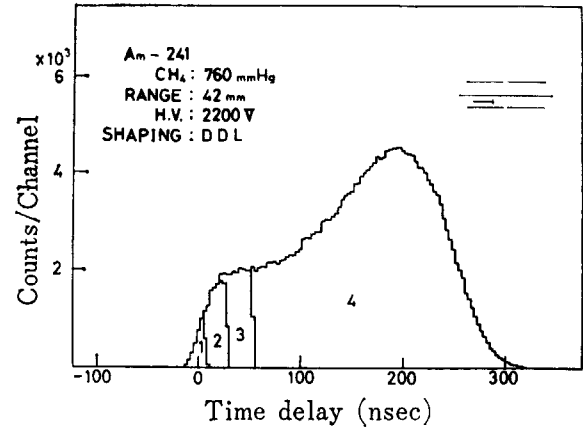


Fig. 23 Effect of the resolving time on the time-distribution (DDL pulse shaping).

axis, approaching to the center wire, (2) parallel to the axis, and (3) similarly inclined but leaving the center wire. It is seen that the DDL shaping (Fig. 21 (a)) gives a somewhat sharper distribution than the RC shaping (Fig. 21 (b)). The point of true coincidence (zero time delay) has been obtained using a pulse generator. The results reveal how particles incident parallel to the center wire will produce the simultaneous outputs from the counters A and B. In the interpretation of the results, however, the effects of collimator opening of  $30^\circ$  and a range of 42 mm must be taken into account. The broadening of the peak observed in the case (3) is caused by the particles passing through the vicinity of cathodes. These results clearly indicate that the present method, by which only particles generating signals simultaneously at the counters A and B are detected, could be successfully applied for the purpose of particle collimation without a collimator.

Figure 22 shows the time distribution of signals B with reference to signals A with and without collimator, obtained through DDL shaping. Spectra (1), (2), (3) and (4) correspond respectively to the collimator openings ( $2\theta$ ) of  $30^\circ$ ,  $50^\circ$ ,  $60^\circ$  and without collimator. The curves reveal how the particles more narrowly collimated in the direction of the axis produce a distribution more closely gathered around zero time delay, thus illustrating how selecting the signals to those around zero time delay could bring about the same effect as collimation parallel to the axis. The dragging tail of the curves, giving them an asymmetrical configuration, would appear to be due mainly to the geometry of the source. A similar result has been observed previously<sup>68</sup>.

In Fig. 23 are presented the effects of differences in the resolving time of electronic collimation on the time distribution with DDL shaping. Spectra (1), (2), (3) and (4) correspond respectively to coincidence limit of 5, 50, 100 nsec and without coincidence. The asymmetry of the curves is due to the absence of particles corresponding to the negative flank of the peak; flanks are to be superimposed on each other irrespective of coincidence cut-off. A comparison of Fig. 23 with Fig. 22 brings out the similarities and differences between electronic collimation and conventional collimation: While the same part of the time distribution is analyzed in both methods, electronic collimation results in a sharper cut-off as compared with the collimator. An opening of  $60^\circ$  of the collimator corresponds roughly to an electronic collimation of 100 nsec.

To demonstrate the results obtainable with the present method, energy spectra were measured with and without electronic collimation for DDL shaping (see Fig. 24). The resolving times of the coincidence were 5, 50 and 100 nsec. For the comparison with Fig. 24, energy spectra with and without collimator are shown in Fig. 25. Three collimators with openings of

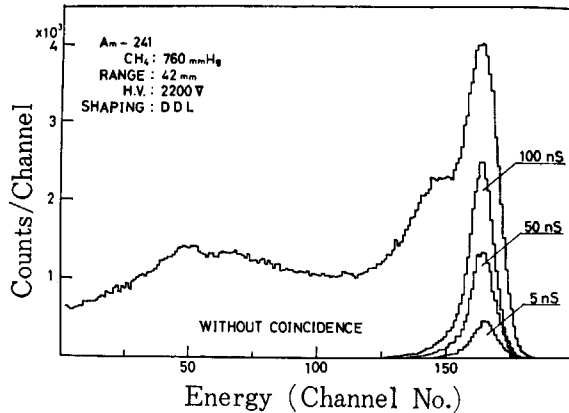


Fig. 24 Energy spectra with and without electronic collimation (DDL pulse shaping).

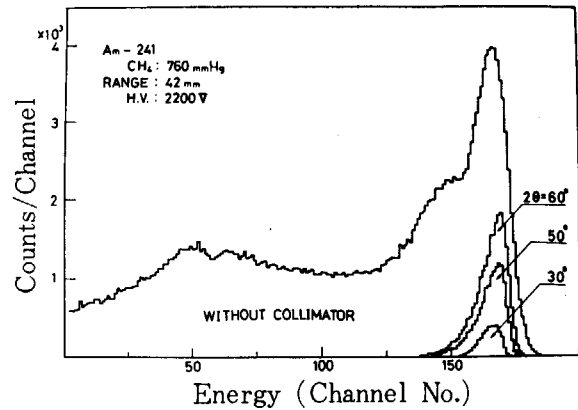


Fig. 25 Energy spectra with and without collimator (DDL pulse shaping).

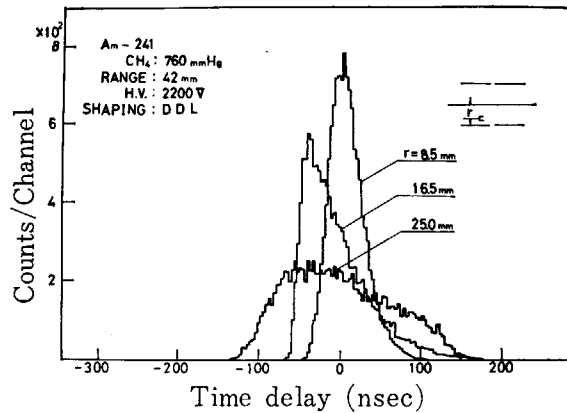


Fig. 26 Effect of the anode-to-source distance ( $r$ ) on the time-distribution.

30°, 50° and 60° were used. The attenuation due to loss of alpha energy through the collimator has been corrected in Fig. 25. Strictly speaking, direct comparison of intensities between the different collimators is not truly valid, because the same areas are not masked by these collimators.

Now, comparing the spectra (1), (2) and (3) in Fig. 21, it would be suspected that particle position (distance from the center wire) should have some effect on the collimating properties. This effect is illustrated in Fig. 26 for DDL pulse shaping using a collimator of 40° opening ( $2\theta$ ). Broadening of the spectra is observed accompanying the increase of distance ( $r$ ) from the center wire to the source. This broadening results from slower drift velocity in the vicinity of the cathodes where the electric field is weak. Such a phenomenon is foreign to the collimator. Thus with electronic collimation there might be a zone, immediately adjoining the cathode, where performance is impaired, and which in some cases might produce false coincidences (see Figs. 21 and 26). The extent of this zone will depend strongly on the gas multiplication factor. On the other hand, the use of an ionization chamber, for which the gas multiplication factor is unity, would eliminate this problem. The lateral shift of the peak position along the time axis, seen in Fig. 26, is due to the geometry of the source.

### 3. 2. 4 Application to the neutron spectrometry<sup>69)</sup>

The present method of electronic collimation described afore is suitable for the use in a gas recoil fast neutron spectrometer. The performance of this type of neutron spectrometer

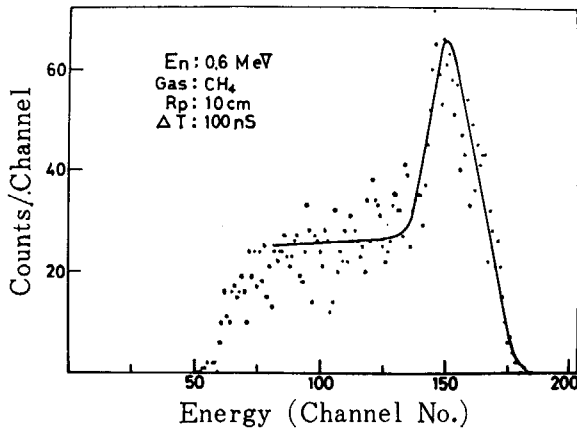


Fig. 27 Response of the spectrometer for 0.6 MeV neutrons (fast coincidence method).

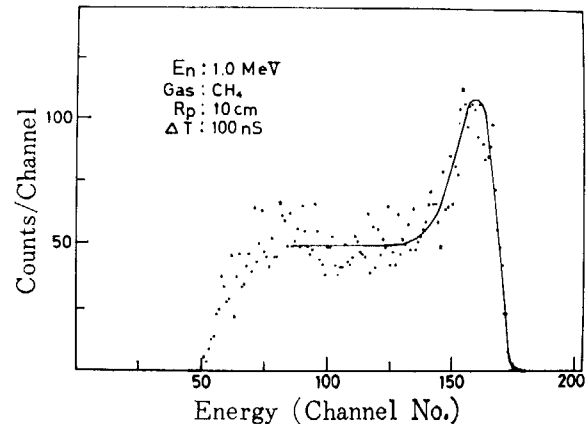


Fig. 28 Response of the spectrometer for 1.0 MeV neutrons (fast coincidence method).

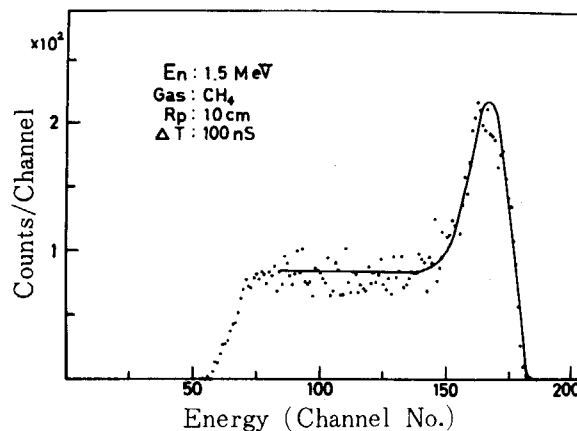


Fig. 29 Response of the spectrometer for 1.5 MeV neutrons (fast coincidence method).

was examined for monoenergetic (p-t) neutrons. A rather thin tritium target was used in this experiment so that the spread in neutron energy was estimated very small ( $\pm 10$  keV), and the neutron yield was alternatively low. The energy spectra obtained for 0.6, 1.0 and 1.5 MeV neutrons are shown in Figs. 27, 28 and 29, respectively. In these experiments, a discrimination level of timing SCAs in each channel A and B was set at 1 volt (20% of the maximum input). This rather high level was required to discriminate electric noises in the target room. It was also high enough to reject false coincidences due to the interaction between counters A and B. A third cathode<sup>67)</sup>, which would be needed to remove the interaction pointed out in section 3. 1, is therefore not introduced in the present experiments.

The gas pressure was chosen so that the range of head-on protons to be 10 cm. In section 3. 1. 8, it was pointed out that the efficiency of this type of neutron spectrometer depends on proton range, being maximum at the same proton range as an effective cathode length. The counter faced the target with the distance of 5 cm in the direction of zero degree. In this set-up, the effective center of counter was 13 cm distant from the target. Neutrons under these conditions may be taken to be approximately in a parallel beam because a recoil within  $\pm 20^\circ$  can be taken for a head-on recoil in the application of this kind of gas recoil neutron spectrometer (assuming an energy resolution of 10%).

The resolving time in coincidence was fixed to 100 nsec throughout the neutron experiments because the reduced resolving time did not improve the peak-to-background ratio but lowered the counter efficiency. Studies on the possible lower limit of coincidence, however, are important as the faster coincidence is necessary in the high-resolution applications.

Each spectrum in Figs. 27~29 had a continuum which was nearly-uniformly distributed from zero to maximum energy. The lower energy region of the continuum, however, was dropped because of the discrimination level in the SCAs. The origin of this continuum seems to be an insufficient volume<sup>67,68)</sup> immediately adjoining to the cathodes; the continuum was estimated too large to be caused by chance coincidences. This conjecture is supported by Photo. 6 in the following section.

### 3. 2. 5 Conclusion

It may be concluded that this method of electronic collimation can offer a new technique for particle collimation to be used in proportional counters and other detectors. A collimating performance similar to conventional collimator can be obtained.

The experiments with an alpha source were masked by disturbance of the electric field caused by the source and source holder, and efforts were directed to minimize this effect. Quantitative estimation of the effects is difficult. The range of alpha particles were set at 42 mm (range in methane at 1 atm.) throughout the experiments. Should there be a change in this range (through the adoption of a different gas pressure or particle energy) or in the applied voltage, this would necessitate an accompanying re-adjustment of the system to obtain the same collimating performance.

The new method of electronic collimation has been used almost successfully in a gas recoil fast neutron spectrometer of the medium radiator type. It is to be noted that the dispensation with the collimator, adopting the present method of electronic collimation, is an important improvement in the neutron spectrometer concerning the background reduction.

The preliminary investigation on the spectrometer gave good results for monoenergetic neutrons of 0.6~1.5 MeV. However, more detailed studies are necessary on the origin of a background continuum observed in the neutron spectra and its dependence on the gas multiplication factor: It is needed for the estimation of the counter efficiency though the continuum can be removed by introducing a rise-time discrimination (refer chapter 4).

## 3. 3 Electronic collimation in a proportional counter by rise-time discrimination<sup>68)86)</sup>

### 3. 3. 1 Introduction

Recent developments in pulse shape discrimination offer a new approach to the collimation by electronic discrimination for use in the proportional counter. This possibility does not appear to have been discussed in literature except for several authors<sup>70)</sup> who have reported on rise time discrimination between different ionizing particles. This section deals with a new method of electronic collimation making use of a rise-time analyzer, which is easy to apply to neutron spectrometers.

In the counter telescope based on the detection of recoil protons with a proportional counter, the most commonly adopted method to collimate the protons is by collimating holes. The transparency of this kind of collimator was 72% in the case of Perlow's<sup>58)</sup> and 40% in the case of the present author's<sup>62)</sup>. The highest transparency of 100% will be realized by electronic collimation. The electronic collimation, furthermore, does not have the drawback of providing a source of background in the neutron field, posing problems in the choice of collimator material.

### 3. 3. 2 Principle of the method

The output pulses from a proportional counter vary in rise-time, as seen in Photo. 3. The

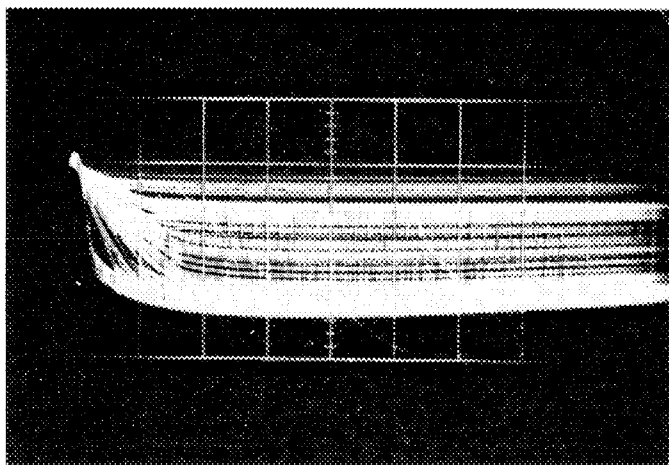


**Photo. 3** Output pulses from a proportional counter after preamplifier for alphas without any collimation. Source;  $^{241}\text{Am}$ , counter gas;  $\text{CH}_4$ -760mmHg, applied voltage; 2200V. Scales; 0.02V/div. and 0.5 $\mu\text{sec}/\text{div}$ .

rise-time should be in principle small for pulses caused by the ionizing particles incident parallel to the counter axis (anode), and large for pulses from particles with other directions. This provides the basis for a new approach to electronic collimation. By selectively detecting pulses of the fastest rise, only particles incident parallel to the counter axis will be detected. By this means a proportional counter can be used as a neutron spectrometer selectively detecting the head-on protons caused by neutrons incident parallel to the counter axis. An alternative method would be to detect all pulses without any collimation, and to apply mathematical operation between the pulse-height and rise-time of each pulse.

The method mentioned first would appear the simpler of the two, though it would have a lower efficiency, while the second method should require some study to work out on the mathematical operation, upon which it could be expected to provide a high efficiency. The present subject is limited to the former method.

### 3. 3. 3 Apparatus

#### (1) Electronics

A block diagram of the electronic collimation system is shown in Fig. 30. The JAERI model 156 linear amplifier<sup>71)</sup> is a spectroscopy amplifier with variable active filters, and is used for energy analysis with 0.8  $\mu\text{sec}$  shaping. The JAERI model 131 linear amplifier<sup>72)</sup> is a multi-mode amplifier with variable RC and DL shaping, and is used for rise-time analysis without any pulse shaping.

The rise-time analyzer is composed of two parts. One is a rise-time to pulse-height converter (RHC) and the other a single-channel pulse height analyzer (SCA). The SCA, Camberra Industries Model 1435, selects the fastest part of the rise-time spectrum. The RHC, JAERI

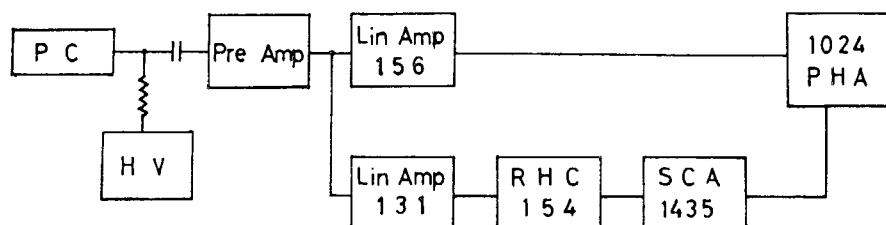


**Fig. 30** Block diagram of the circuit (rise-time method).

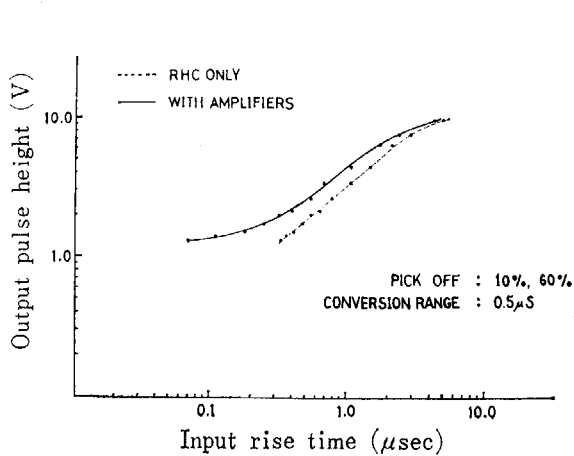


Fig. 31 Linearity of the rise-time-to-pulse-height converter (RHC).

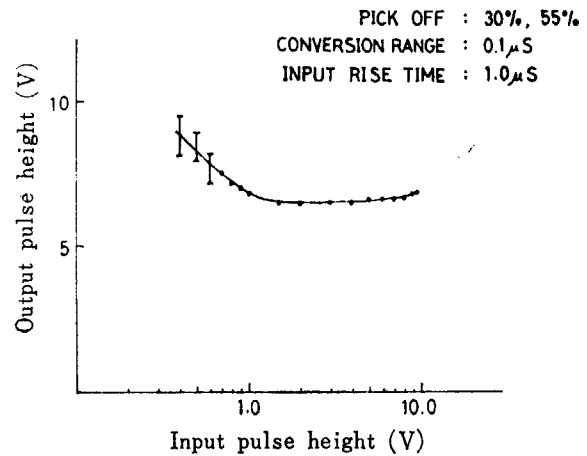


Fig. 32 Dependency of RHC output on the input pulse-height.

model 154<sup>74)</sup>, has two fractional pulse height discriminators (lower pick-off and upper pick-off) and their levels can be varied from 0% to 100% of the input pulse height. The interval between the two pick-off signals is converted to pulse-height by means of the time to pulse height converter. The conversion range of the converter (the maximum time interval corresponding to the maximum output pulse height) can be selected in the range from 100 nsec to 10  $\mu$ sec. The RHC has also two discriminators (lower and upper) to select the pulses to be analyzed. Details of the converter are described in ref.<sup>74)</sup>

The performance of the RHC is shown in Figs. 31 and 32. Figure 31 plots the output pulse height against input rise-time. The thin broken line represents the output of the RHD only, while solid line is for the whole system including pre-amplifier and linear amplifier. Figure 32 relates the RHC output to the height of input pulse with a constant rise-time. Significant deviations are observed in the lower input region, and the lower discrimination level was therefore set at 1.0 V in the present experiments.

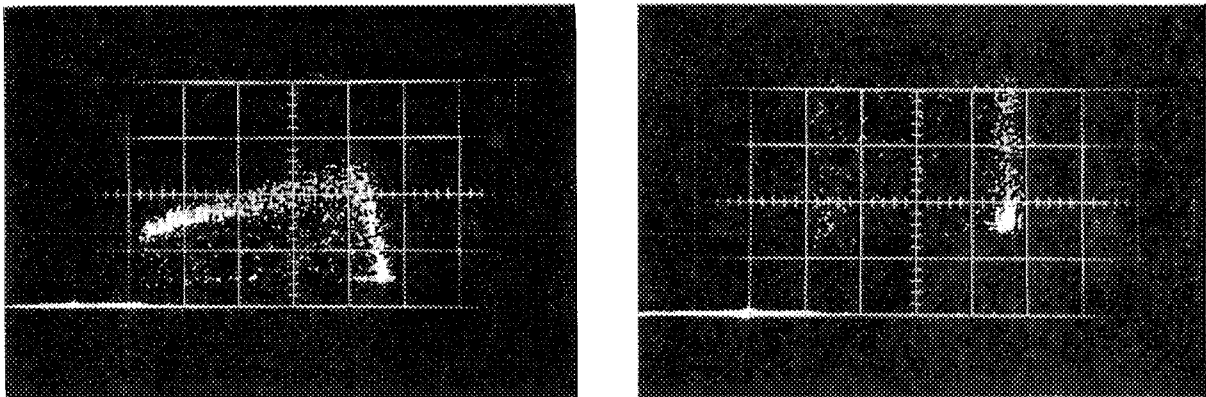
## (2) Counter

The counter is a methane-filled proportional counter with an anode of 0.05 mm diameter and a cathode of 62 mm innerdiameter. The cathode is insulated from the counter vessel to permit the anode to use at zero potential. The counter vessel and cathode are made of aluminum (A-1 B) and the anode wire is stainless steel. There is no guard ring in the counter, and field definition was obtained with syringes of 0.6mm outer diameter. To reduce water vapor in the counter gas a  $Mg(ClO_4)_2$  trap was used.

### 3. 3. 4 Measurements and discussions

To ascertain the possibility of electronic collimation by rise-time discrimination and to obtain some indication of the performance that would be expected, preliminary measurements were conducted using alpha particles from an <sup>241</sup>Am source.

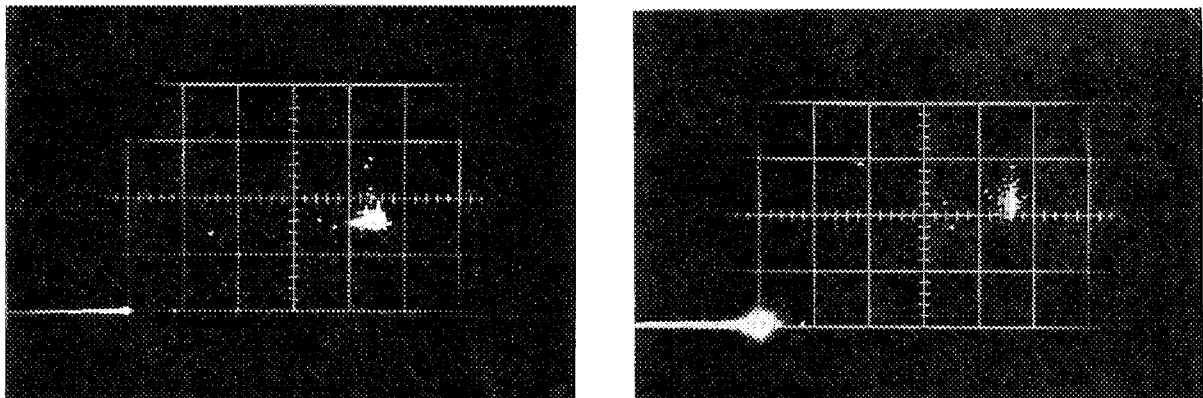
Photograph 3 gives examples of the shapes of the output pulses from the pre-amplifier. The source plate was placed without collimator in a proportional counter filled with 1 atm. of methane. Pulses of different rise-time are observed on the oscilloscope even when only those with maximum pulse-height (corresponding to particles which have lost their entire energy in the gas) are compared. It is quite reasonable to suppose that the fast pulses correspond to the particles traveling parallel to the counter axis and the slow ones to the other particles.



(a)

(b)

**Photo. 4** Two-dimensional display of energy (abscissa) *vs.* rise-time (ordinate) for alphas without any collimation. (a) Scales; energy (abscissa) 1 MeV/div. risetime (ordinate) 1  $\mu$ sec/div. RHC pick-off levels; 30 and 60%, conversion range; 0.5  $\mu$ sec. Applied voltage; 2200V. (b) Scales; Energy 1.2 MeV/div., risetime 0.15  $\mu$ sec/div. RHC pick-off levels; 30 and 50%, conversion range; 0.1  $\mu$ sec.



(a)

(b)

**Photo. 5** Two-dimensional display of energy (abscissa) *vs.* rise-time (ordinate) for conventionally collimated ( $2\theta=30^\circ$ ) alphas. Scales; same as in **Photo. 4** (b). RHC pick-off levels; 30 and 55%, conversion range; 0.1  $\mu$ sec. Applied voltage; 2200V. (a) Parallel to center wire. (b)  $30^\circ$  with respect to center wire.

**Photographs 4** (a) and (b) are two-dimensional dots-on-film display, relating pulse-height on the abscissa to rise-time on the ordinate, without any collimation. The range of the particles was set at 42 mm throughout these experiments. The observed interval of rise-time is entirely covered in **Photo. 4** (a), while in **Photo. 4** (b) the ordinate is magnified by a factor of about 7 to show up details of the fastest part of the rise-time. Particles of maximum energies and fastest rise-times can be taken to be those traveling parallel to the center wire. In **Photo. 4** (a) many particles colliding with the cathode are observed, which are represented by the dots registered at lowered energies and hence at faster rise times. Also there are some particles traveling very close to (or just colliding with) the cathode. They show slightly lower energies attributable to the decreased drift velocity in the counter and the pulse shaping time constants of the amplifier system. They show a wide distribution (from the maximum to the minimum) in rise-time according to their directions.

The introduction of a collimator results in the **Photos. 5** (a) and (b), to be compared with **Photo. 4** (b). In both **Photos. 5** (a) and (b), the collimator opening  $2\theta$  was  $30^\circ$ , while the direction of track was parallel to the center wire in **Photo. 5** (a) and  $30^\circ$  in reference to the wire in **Photo. 5** (b).

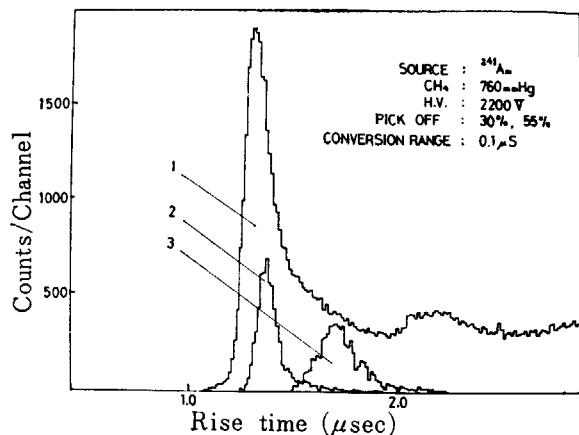


**Fig. 33** Effect of particle direction on rise-time spectrum. (1) without any collimation, (2) collimated ( $2\theta=30^\circ$ ) particles parallel to center wire, (3) inclined  $30^\circ$  with respect to the wire. RHC pick-off; 30 and 50%, conversion range;  $0.1\mu\text{sec}$ .

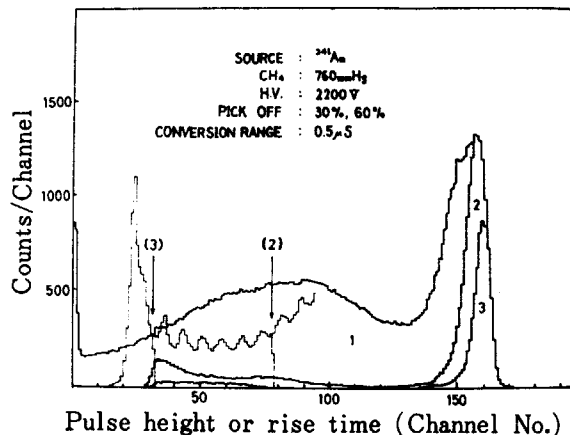


**Fig. 34** Energy spectra with and without rise-time discrimination.

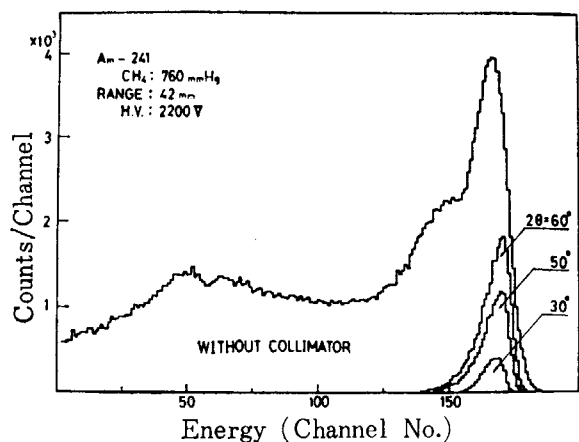


**Fig. 35** Energy spectra with and without conventional collimator.

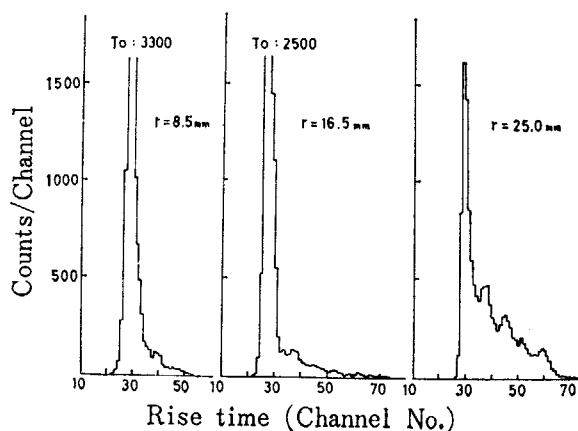


**Fig. 36** Effect of particle position (distance  $r$  from center wire) on the rise-time spectrum.

Rise-time spectra are shown in **Fig. 33**. The spectra (1), (2) and (3) in the figure correspond to **Photos. 4 (b)**, **5 (a)** and **5 (b)**, respectively. Referring to **Photo. 5** and **Fig. 33**, one may have a confirmation of the expectation raised by **Photos. 3** and **4** that the parallel particles exhibit the fastest rise-time and others do not. This constitutes the basic phenomenon on which the present method of electronic collimation is founded.

To demonstrate the effectiveness of this system of electronic collimation, energy spectra were measured with and without the collimation (**Fig. 34**) and with and without collimator (**Fig. 35**). In **Fig. 34**, energy spectra 2 and 3 (represented by the thick solid lines) correspond respectively to the cut off levels (2) and (3) indicated in the rise-time spectrum (thin solid line), while the spectrum 1 is the original untrammelled energy distribution. These were obtained with the counter filled with 1 atm. of methane and with an applied voltage of 2,200 V. The gas multiplication factor under these conditions was estimated to be 25, and was maintained constant throughout the experiments. For the comparison with **Fig. 34**, energy spectra obtained with and without collimator are shown in **Fig. 35**. Three collimators with openings of  $2\theta=30^\circ$ ,  $50^\circ$  and  $60^\circ$  were used. The alpha energy was attenuated in the passage through the collimator, and this attenuation is corrected in **Fig. 35**. But direct comparison in terms of absolute intensities can be misleading, because different areas are masked according to the collimator



used. Moreover the disturbance of the electric field by the source and source holder cannot be ignored in detailed discussion. **Figure 34** definitely establishes the practicality of the electronic collimation by rise-time discrimination, for the purpose of selectively detecting particles traveling parallel to the counter axis in a proportional counter. A comparison between **Figs. 34** and **35**, however, reveal some differences in effect between electronic collimation and collimator. Energy spectra with electronic collimation result in sharp distributions in the peak profile but are accompanied by a trail of low lying hills in the lower pulse-height region. The origin of the redundant spectrum is not well understood (or estimated). Referring **Photo. 4 (a)** it is clear that alpha particles colliding the cathode do not provide such a fast rise-time. A possible origin is the performance of the electronics (especially the RHC) at high pulse rate.

In **Fig. 36**, rise-time spectra are shown for particles collimated to  $2\theta=40^\circ$  and with a range of 42 mm. Upon increasing the distance ( $r$ ) between the counter axis (anode) and source, the trailing tail at the longer end of the spectrum is seen to be growing. From these results one may say that the tail is caused by particles passing the neighborhood of (or colliding with) the cathode: electrons produced in the vicinity of the cathode in a proportional counter move very slowly towards the center wire, the electric field being weak in this region. They take a longer time to reach the gas multiplication region causing deviations in drift time required by individual electrons. This means that particles traveling close to the cathode and with a direction slightly oblique to the counter axis cannot produce fast rise pulses. So the volume in the immediate vicinity of the cathode will not possess very effective collimating properties. The extent of this insufficient volume will depend on the electric field of the counter, and this is consistent with previous findings<sup>67)</sup>. It is to be noted, however, that a collimator too does not offer the required properties in the immediate neighborhood of the collimator. The collimating properties would predominantly depend on the drift velocity of electrons, and re-adjustment of the settings of the system could bring about a required collimating performance for the different counter parameters.

Comparing the present method with the previous one<sup>67)</sup> (section 3. 2), the first and foremost improvement lies in the simpler set-up of the present system. A proportional counter without any specially designed construction can be used and the electronics are also simpler. The linear amplifier 131 in **Fig. 30** is not indispensable, and when omitted, the RHC is fed from the linear amplifier 156. An insufficient volume is expected with both present and previous collimation. In the case of the present (rise-time) method, however, pulses from this volume are rejected because these are with slow rise. This volume, on the other hand, is conducive to false coincidences on recoil protons (in the application for neutron spectrometry) in the case of the previous (fast coincidence) method. This is the second advantage of the present method. The third advantage of the present method is freedom from the problem of the interaction observed between the counters A and B in the previous method, which gave rise to loss and inaccurate estimation of the efficiency. The drawback of the spectra obtained with the present method is the redundant hill (see **Fig. 34**) appearing at the lower end of the spectrum.

### 3. 3. 5 Application to the neutron spectrometry<sup>81)</sup>

Present method of the electronic collimation is suitable to use in a gas recoil fast neutron spectrometer. In this application, a conventional counter construction without any collimator or other special construction can be used for a neutron spectrometer giving a differential spectrum.

Neutrons in this application are incident on the counter from the direction parallel to the anode. Head-on protons are selectively detected by means of electronics as shown in **Fig. 30**. A linear amplifier (model 131) in the figure, however, was replaced by a model 158 dual fast

amplifier as model 131 has an insufficient high-frequency response for this application.

The neutron energy  $E_n$  is directly given by the measured proton energy  $E_p$  as the recoil angle  $\theta$  in the well-known relationship  $E_p = E_n \cos^2 \theta$  is zero ( $\theta \approx 0$ ) in this case. An observed  $E_p$  spectrum, however, does not give the true neutron spectrum; an  $E_p$  spectrum is always accompanied with large angle recoils in the lower energy region. These recoiling protons with a large recoil angle and a short range are undesirable but inherent in this collimation scheme. They are understood as follows:

Figure 37 (a) represents a polar plot of the track lengths for recoiling protons originating at the point A due to a beam of neutrons parallel to the anode. On the other hand, a rise-time of the output pulse depends on the radial component of the track length. An example of the discrimination level in rise-time is shown in Fig. 37 (a) by the two solid lines parallel to the neutron direction. By the rise-time discrimination in the present scheme, proton recoils are

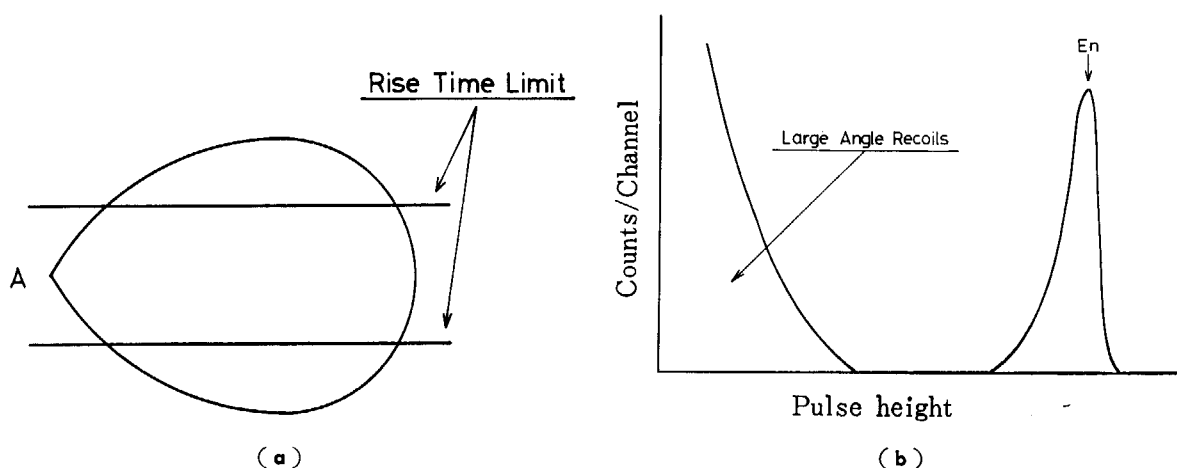


Fig. 37 Principle of electronic collimation (rise-time method)

(a) Rise-time limit in recoil track lengths.

(b) Schematic distribution of the pulse-heights in rise-time method.

divided into three groups; (1) those with a longer radial component than discrimination level (rise-time limit), so that they are rejected, (2) those with a small radial component (rise-time) but large recoil angle giving undesired outputs (large angle recoils) and (3) those with a small rise-time and small recoil angle ( $\theta \approx 0$ ) giving desired outputs (neutron energy). In Fig. 37 (b), the pulse height spectrum obtainable with the present method of electronic collimation is shown schematically. It is similar in shape to that obtainable in a Giles' collimating scheme.

Ideally saying, the intermediate region of the pulse height spectrum between a desired peak and a corresponding large angle recoil spectrum should be free of pulses. Origins of these valley pulses were pointed out by BENESON *et al.*<sup>17)</sup> to be (1) recoils striking cathod wires, (2) recoils penetrating the screen cathod but failing to be detected in the outer (anti-coincidence) counters due to any impairment of the outer counter ability, (3) end effect in the central (main) counter and (4) neutrons scattered before entering the central volume. The present method of electronic collimation seems to be advantageous in this respect especially in items 1) and 2).

Moreover, a collimation in this method can be adjusted to a desired degree (strict or lenient) without any change in the counter parameters; it is easily adjusted by setting parameters in the rise-time analyzer. In the Giles spectrometer, it is necessary to change the gas pressure for the different degrees of the collimation. It is much preferable as compared with a conventional spectrometer in which a complicated procedure was needed to change counter parameters.

The difference in characteristics between the present method and the collimator is that with the former the effective collimation varies according to the distance from anode, whereas such kind of space dencence does not occur with the collimator. On the other hand, the effectiveness of the collimator impaired for proton recoils produced at short distance from the collimator and this shortcoming is conversely not shared by the electronic collimation.

A gamma rejection in this method may be excellent because the majority of gamma pulses will be due to electrons from the cathode material. They are fortunately not analysed as they are impossible to produce fast-rise pulses. This rejecting property for the gamma pulses is also useful for neutron-gamma discrimination in a gas recoil spectrometer of the type giving an integral spectrum (refer Chapter 4).

Performance of the spectrometer was examined using a beam of monoenergetic (p-t) neutrons of 0.6~1.5 MeV. A very thin tritium target was used, so the energy spread of incident neutrons was estimated to be only  $\pm 10$  keV. The counter was placed so that the center of effective volume (18 cm long) of the counter was 20 cm distant from the target in the  $0^\circ$  direction. A proton range of  $\sim 5.0$  cm was chosen referring a cathode diameter 6.2 cm in the experiments.

In Figs. 38, 39 and 40, pulse height spectra are shown for neutrons of 0.6, 1.0 and 1.5 MeV, respectively. An energy resolution of  $\sim 8\%$  was obtained for 1.5 MeV neutrons for example, and a better resolution will be obtainable by re-adjusting the parameters in a rise-time channel.

In the case that the large angle recoils make any troubles, they will be easily removed by

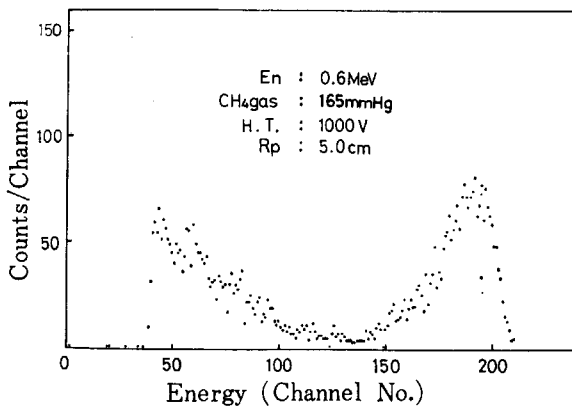


Fig. 38 Response of the spectrometer for 0.6MeV neutrons (rise-time method).

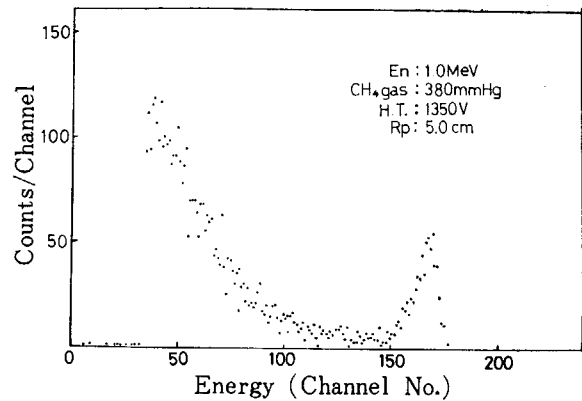


Fig. 39 Response of the spectrometer for 1.0 MeV neutrons (rise-time method).

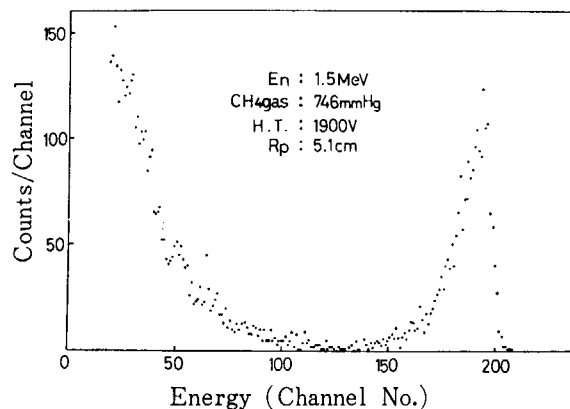


Fig. 40 Response of the spectrometer for 1.5MeV neutrons (rise-time method).

introducing a coincidence between counters divided by means of divided cathodes or anodes<sup>57)67)</sup>.

Each spectrum in the figures is accompanied with appreciable valley pulses though the reduced valley pulses are theoretically expected in this method. Possible origins of the valley pulses are not well understood but one of them seems to be an insufficient volume in the vicinity of the cathode.

### 3. 3. 6 Conclusion

Experiments with an alpha source have proven the feasibility of the present method for electronic collimation based on rise-time discrimination in a proportional counter. It showed a sharper collimation compared with the collimator, however, the spectra are accompanied with a redundant hill.

The present experiments show that detailed studies are necessary in a more precise application because, (a) the rise-time of output pulse will depend on the gas multiplication and on the track location (distance from the anode), b) an insufficient volume pointed out in the present studies<sup>67)68)81)</sup> will also depend on the gas multiplication and, in the worst case, it may be unavoidable in this method.

However, a possibility of removing the insufficient volume (in the other term, the valley pulses in the neutron spectrometer) is to be noted: The volume is due to the slower electron drift velocity at the vicinity of the cathode. The electron drift velocity, however, can be kept constant (independent of  $r$ ) in a proportional counter using a suitable gas mixture. The volume is reduced or removed in such a counter.

The new method of electronic collimation was successfully applied in the preliminary studies on a gas recoil neutron spectrometer. The most notable improvement is the simplification obtained on the instrumentation (counter and electronics). Moreover, a spectrometer with the present method of collimation has inherent low gamma sensitivity.

The dispensation with a collimator by using the present method of electronic collimation (rise-time collimation) brought following advantage; a) the method is perfectly free from difficulties<sup>62)</sup> in the choice of material and machining of the collimator, b) freedom from the background due to a collimator which should be placed in the counter and c) a degree of collimation, which depends on a required energy resolution, is easily adjustable by the settings in a electronic system without any resetting in the counter parameter.

The large angle recoils are inherent in the Giles' collimation scheme and the present one. However, these are removed by combining the present method with the previous one<sup>57)67)</sup> as will be described in section 3. 4.

## 3. 4 Combined method of the two foregoing methods

### 3. 4. 1 Introduction

Defects in the two foregoing methods, the continuous background in the fast coincidence method and large angle recoils in the rise-time method, are expected to be removed by combining two methods. Two features of combination are possible in which a method provides with the collimation and the other removes the defects. A rise-time method combined with a coincidence method can be taken as an application of the technique by the author<sup>57)</sup>, which removed large angle recoils in a Giles' spectrometer.

### 3. 4. 2 Results and discussions

An example was presented for the coincidence method combined with a rise-time discrimi-

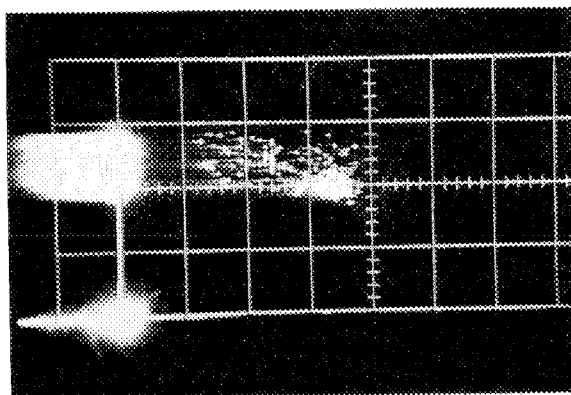


**Photo. 6** Two-dimensional display of energy (abscissa) *vs.* rise-time (ordinate) in the spectrometer (coincidence method). Neutron energy; 1.5 MeV, scales; 0.4MeV/div. and 100nsec/div.

nation. The conjecture that the origin of a background continuum may be an insufficient volume immediately adjoining to the cathodes, was supported by **Photo. 6**. In the photograph, the relation of energy (abscissa) and rise-time (ordinate) in the fast coincidence method is displayed two-dimensionally, using an apparatus described in the previous section<sup>67,68</sup> (refer **Photos. 1, 2, 4 and 5**). In this experiment, input signals of the PHA were; the energy signals on the F-side ADC, the rise-time signals (refer to **Fig. 30**) on the M-side ADC and the coincidence signals (refer to **Fig. 20**) on the coincidence gate. In the rise-time channel, however, the linear amplifier model 131 in **Fig. 30** was replaced by the model 158 dual fast amplifiers and the SCA 1435 was removed.

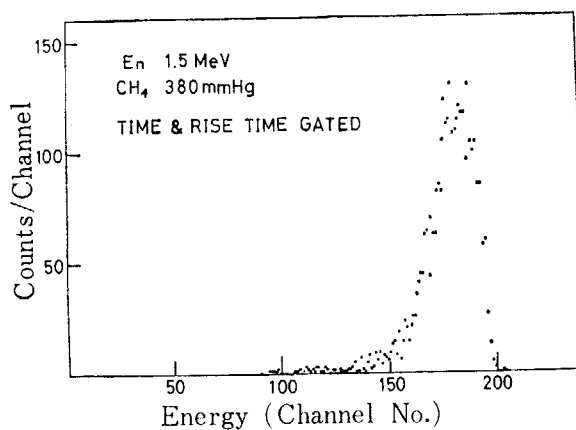


**Fig. 41** Response of the spectrometer for 1.5MeV neutrons (fast coincidence method combined with rise-time discrimination).

In **Photo. 6**, protons corresponding to the continuum represent slower rise-times than those in the true peak. Making use of this effect, the continuum was perfectly removed by introducing a rise-time discrimination described in section 3. 3. The RHC in this application was followed with a SCA (single channel pulse height analyser) and pulses with the fastest rise-time were selectively detected. The SCA was also equipped with delay and gate generators. Gating the energy signal with this rise-time gate, an energy spectrum (coincidence and rise-time gated) was obtained for 1.5 MeV neutrons as shown in **Fig. 41**. As seen in the spectrum, undesirable pulses from an insufficient volume immediately adjoining to the cathode were removed due to its slower rise-time.

### 3. 5 Electronic collimation with rise-time discrimination in a gridded ionization chamber

#### 3. 5. 1 Introduction

In the study of rise-time collimation in a proportional counter<sup>68)</sup>, it was pointed out that there is an insufficient volume, which would be reduced at the high gas-multiplication or would not be observed in a ionization chamber in which the gas-multiplication is unity. The electronic collimation, therefore, was studied with a gridded ionization chamber using a rise-time method<sup>82, 83)</sup>.

The output pulses of an ionization chamber give a variety of information on the detected radiation under investigation. Generally, however, only the amount of ion pairs is interested in energy measurements, for example.

In a parallel-plate type ionization chamber, electrons along the track of a charged particle drift in the direction of the electric field and collect on the anode (collecting electrode) without serious track deformation. That is, the output pulses provide the information on particle range, specific ionization, orientation and location of the track, and drift velocity. Several papers are available on the measurement of orientation of a track.

VOROB'EV, KOMAR and KOROLYOV<sup>75, 76)</sup> used pulses from the grid in a gridded chamber as a measure of the angle  $\theta$  between particle track and electric field. They collimated the charged particles by selecting only the grid pulses corresponding to  $\theta=0$  with a single channel pulse height analyzer (SCA). The energy resolution was improved by this collimation, and the 14 keV of fwhm was realized for alpha particles from <sup>224</sup>Ra. However, the fluctuation in grid potential affected the anode pulses due to electrostatic induction and the energy resolution was impaired. The energy resolution of 14 keV was achieved by a strict collimation resulting in a low transparency of collimation or efficiency of the chamber.

If, then, a chamber could be obtained in which the fluctuation of grid potential did not affect the energy resolution, the high efficiency of the chamber would be realized together with the high energy resolution.

DÖKE, OGAWA and TSUKUDA<sup>77~79)</sup> constructed such a chamber by introducing an additional (the second) grid for angle information. In this double-gridded chamber, an electric potential did not fluctuate in the first grid which faced the anode. This means that the chamber could be used with a higher efficiency than that by VOROB'EV *et al.*

On the other hand, FACCHINI *et al.*<sup>80)</sup> used the difference in shape of the output pulses in

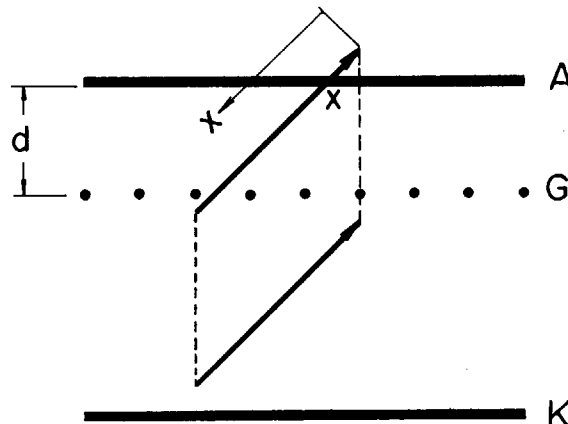


Fig. 42 Schematic drawing for pulse-shape analysis in a gridded ionization chamber.

an conventional gridded chamber as the angle information ; the current pulses from the anode had different rise-times according to the angle  $\theta$ . The outputs from a pre-amplifier were fed to two channels ; the energy channel was an amplifier system with a delay line (DL) clipping of  $8 \mu\text{sec}$ , and the angle information channel was with a DL clipping of  $0.5 \mu\text{sec}$ .

In the present method using a rise-time to pulse-height converter<sup>74)</sup> (RHC), the difference in rise-time of the output pulses from a conventional gridded chamber is used. By this method, the vagueness in the information given by the above method can be eliminated, and flexibility is also given in the choice of information. In this chapter, characteristics of the angle information are described, and also some applications of the information.

3. 5. 2 Principle of the method

To analyze the rise-time of output pulses from a gridded ionization chamber, it is convenient to deal first with the current pulses. Electrons drift and arrive at the grid, the output current is started in the anode circuit, and it then disappears with sweeping of all electrons to the anode. The current  $i(t)$  corresponds to the number of electrons in the volume between anode and grid. It is written as

$$i(t) = \frac{w_-}{d} \int_{x(t)}^{x(t)+d/\cos\theta} \rho(x) dx, \quad (\rho(x)=0 \text{ for } x < 0, x > R) \tag{14}$$

where  $t$  is the time elapsing after arrival of electron at the grid,  $w_-$  the electron drift velocity,  $d$  the distance between anode and grid,  $x$  a length measured from the end of the track,  $\theta$  the angle between track and direction of the electric field,  $\rho(x)$  the linear density of charge at point  $x$ , and  $R$  is the range of a particle. Then, the voltage output  $v(t)$  is given as

$$v(t) = \frac{1}{C} \int_{t=0}^t i(t) dt, \tag{15}$$

where  $C$  is the capacity of the detector system. The peak pulse height  $v_0$  is given by

$$v_0 = \frac{1}{C} \int_{t=0}^{(d+R \cos \theta)/w_-} i(t) dt. \tag{16}$$

Pulse shapes of the current and voltage outputs for different  $\theta$  ( $\theta_1$  and  $\theta_2$ ) are shown schematically in Fig. 43. From the figure, it is seen that the angle  $\theta$  can be estimated from information on the rise-time of output pulses either of current or voltage.

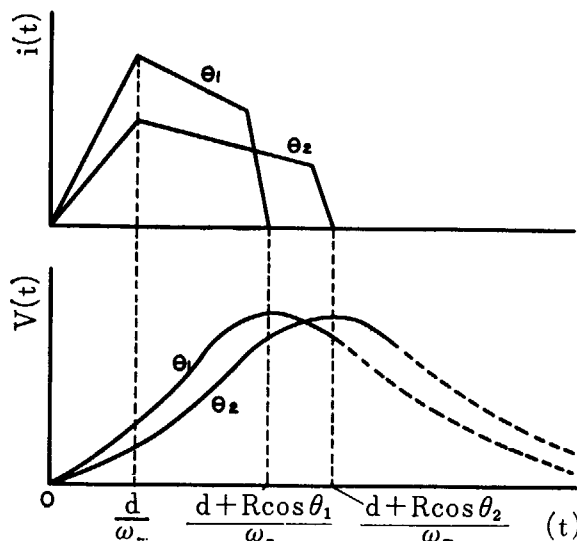


Fig. 43 Schematic shapes of current and voltage pulses in a gridded ionization chamber.

### 3. 5. 3 Experimental apparatus

#### (1) Ionization chamber

The gridded ionization chamber was filled with a mixture of argon (90 %) and methane (10 %) at 1 atm. The distance between anode and grid was 30 mm, and that between grid and cathode 50 mm. The diameter of the cathode was 150 mm. The grid was an arrangement of parallel stainless steel wires of diameter 0.01 mm at 1 mm intervals. The inefficiency of screening of the grid was estimated to be less than 1 %. The ionization chamber was operated with the anode at an earth potential, the cathode at a negative high voltage and the grid at 70 % of the cathode potential. In the present article, "applied voltage" means the cathode potential. For measurement of the rise-time, the applied voltage must be stable and reproducible, because the drift velocity of electrons depends strongly on the electric field, whereas the energy (total charge) is not influenced by the applied voltage unless it is too low.

#### (2) Electronics

A block diagram of the electronics used is shown in Fig. 44 ; the model numbers are for

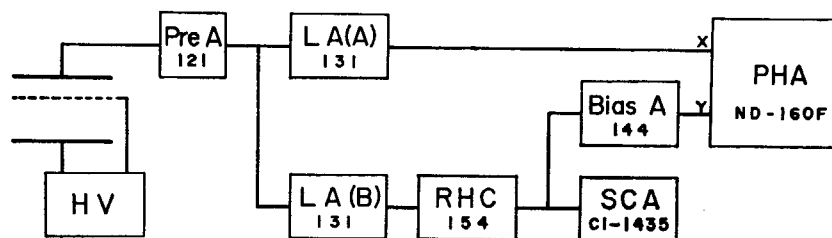


Fig. 44 Block diagram of rise-time collimation in a gridded ionization chamber.

JAERI's unless otherwise indicated. The RHC in the diagram is described in detail in the literature<sup>74</sup>. The output pulses from a charge-sensitive preamplifier are fed to both of the linear amplifiers A and B. The energy information is obtained with the pulse shaping of 5  $\mu$ sec by RC integration and differentiation, while the rise-time information through an amplifier without pulse shaping. The amplifier B can be eliminated, for the output from the amplifier A may be fed to the RHC. Then, similar information is obtained because the rise-time information is retained after the pulse shaping. In certain cases, a biased amplifier (post amplifier) was additionally used to magnify a part of the rise-time spectrum.

#### 3. 5. 4 Measurements and discussions

Characteristics of the angle information were examined as follows. An  $^{241}\text{Am}$  source on the cathode was covered with a thin aluminum foil (2.0 mg/cm<sup>2</sup>). This arrangement gave different energies to the alpha particles with the correspondent different angles  $\theta$ . The purpose of this covering was to simulate proton recoils from a thin radiator in a fast neutron spectrometer. Figure 45 shows the relation between the energy and  $R\cos\theta$  in the arrangement ; the rise-time of output pulses should be proportional to  $R\cos\theta$ .

The energy *vs.* angle information is represented two-dimensionally in Photo. 7, using the apparatus in the refs. 67 and 68. In the photograph, the ordinate is the rise-time scaled to 0.16  $\mu$ sec/div., in which the base line corresponds to 0.48  $\mu$ sec, the abscissa is the energy in the scale of 0.8 MeV/div. The broadening in energy at a given point of the rise-time is caused by insufficient flatness and non-uniformity of the aluminum foil, energy spectrum (dou-



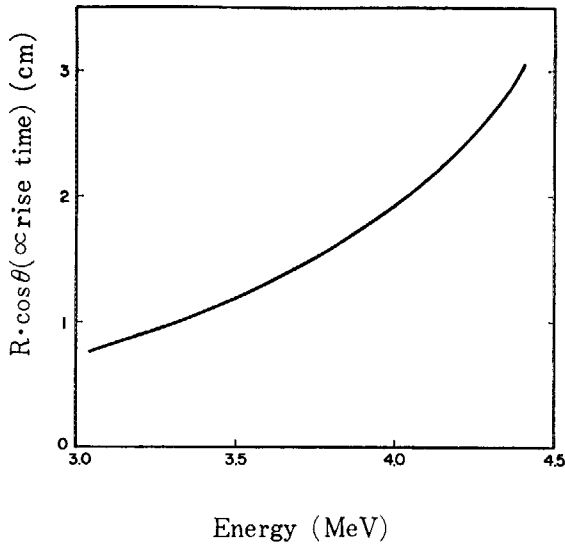


Fig. 45 Energy vs. range component  $R \cos \theta$  for a alpha source covered with an aluminum foil.

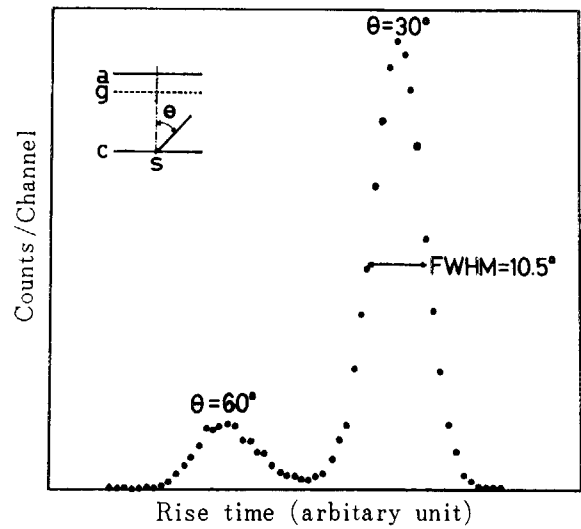


Fig. 46 Rise-time distribution for collimated alphas.

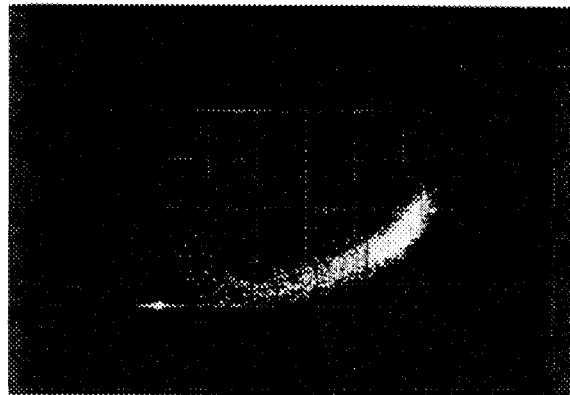


Photo. 7 Two-dimensional display of energy (abscissa) vs. risetime (ordinate) in a gridded ionization chamber. Source ;  $^{241}\text{Am}$  covered with  $2 \text{ mg/cm}^2$  aluminum foil. Applied voltage ; 1200V, scales ;  $0.8 \text{ MeV/div.}$  and  $0.16 \mu\text{sec/div.}$  (base line of the ordinate corresponds to  $4.8 \mu\text{sec}$ ).

ble) of the  $^{241}\text{Am}$ , and performance of the apparatus.

The resolution in angle information is illustrated in Fig. 46. In this measurement, a Ra(DEF) source (5.3 MeV alphas) and a collimator with two holes of  $\theta = 30^\circ$  and  $60^\circ$  directions were used. The resolving power was estimated to be  $10^\circ$  for  $\theta = 30^\circ$  and  $12^\circ$  for  $\theta = 60^\circ$ , assuming that the rise-time was nearly linear for the  $\theta$  in the region of  $\theta = 30^\circ \sim 60^\circ$ . In ref. 80, these values were  $7^\circ$  for  $\theta = 30^\circ$  and  $10^\circ$  for  $\theta = 60^\circ$  with a similar assumption. In Fig. 46 and Photo. 7, it is seen that the method proposed gives good information on the angle  $\theta$ .

### 3. 5. 5 Conclusion

The present method of rise-time analysis with a gridded ionization chamber gives good information on the angle  $\theta$ . It may be applied for obtaining the angle information in nuclear reactions. The present method also provides a neutron spectrometer of the multi-hole collimator type with a thin radiator which was hitherto impossible. In the spectrometer the electronically collimated recoils are utilized, or the majority of recoils are used without a collimation by combining with the rise-time (angle) information.

## 4. Other Applications of the Rise-Time Method

It was shown in chapter 2. how important or, in some cases, unavoidable the neutron-gamma discrimination is in the neutron spectrometers.

This chapter deals with the applications of the rise-time method in the particle discrimination and some related applications; neutron-gamma discrimination in a proportional counter, particle discrimination, reduction of background and large angle recoils, and an application of the particle collimation in a gridded ionization chamber.

### 4. 1 Application to neutron-gamma discrimination in a proportional counter

#### 4. 1. 1 Introduction

A method of neutron-gamma discrimination for a proportional counter was reported by BENNET. A rise-time information, on which the neutron-gamma discrimination was bounded, was obtained by the delay line clipping or by the fast differentiation of the output pulses. A more direct method<sup>(49)(81)</sup> of obtaining the rise-time information is to use an RHC (a rise-time to pulse-height converter). This technique was applied for a gas recoil proportional counter<sup>(84)</sup>.

#### 4. 1. 2 Results and discussions

The relation between energy (abscissa) and rise-time information (ordinate) was displayed two-dimensionally, which shows the possibility of neutron-gamma discrimination. **Photos. 8-a)** and **b)** are for a hydrogen-filled proportional counter illuminated in a gamma (<sup>60</sup>Co) ray field and in a neutron( $\leq 125$  keV)-gamma(<sup>60</sup>Co) mixed field. **Photos. 9-a)** and **b)** are for methane-filled counter in the similar fields. In these figures, neutron events were observed as a peak near the ordinate, representing a narrow distribution in a rise-time compared with gamma events.

Most of the gamma events are due to electrons from the cathode material in the gas proportional counters. By the study described in chapter 3. it was shown that particles in the

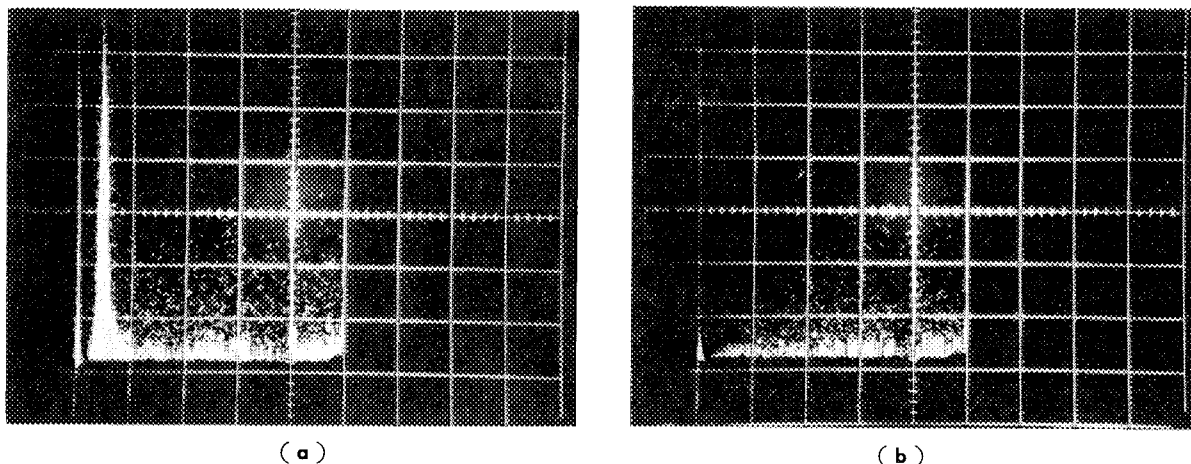


**Photo. 8** Neutron-gamma discrimination in a hydrogen-filled proportional counter (rise-time method). Scales; 100nsec/div. (abscissa) and 20keV/div. (ordinate). RHC pick-off; 5%, and 50%, conversion range; 0.5 $\mu$ sec.  
**(a)** neutrons (125keV) and <sup>60</sup>Co gammas (mixed). **(b)** <sup>60</sup>Co gammas only.

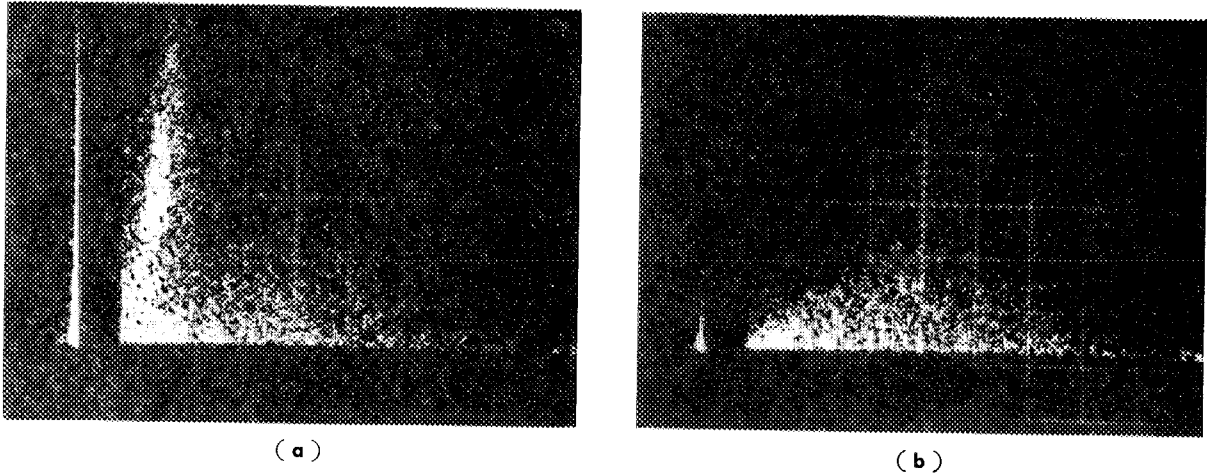


**Photo. 9** Neutron-gamma discrimination in a methane-filled proportional counter (rise-time method). Scales; 10nsec/div. (abscissa) and 85 keV/div. (ordinate). RHC pick-off levels; 5% and 30%, conversion range; 0.2μsec.  
 (a) neutrons (574 keV) and <sup>60</sup>Co gammas (mixed). (b) <sup>60</sup>Co gammas only.

vicinity of the cathode exhibit slow-rise outputs. This fact emphasizes the rise-time difference between gammas and recoil protons. In spite of the straightforwardness of this method, a sharp cut-off was not shown, and was inferior to Bennet method at this stage.

#### 4. 2 Application to the particle collimation and discrimination in a gridded ionization chamber

##### 4. 2. 1 Introduction

Several methods of neutron-gamma discrimination use a difference in particle range. Discrimination properties were examined with a gridded ionization chamber. Alpha sources were used to simulate neutrons (protons) against gammas (electrons), background neutrons, large angle recoils, or carbon recoils.

##### 4. 2. 2 Applications

###### (1) Beta discrimination (neutron-gamma discrimination)

Beta particles cause background in an alpha spectrometry. However, this is easily eliminated by the present method because beta particles have long ranges, hence slow rise-times. To

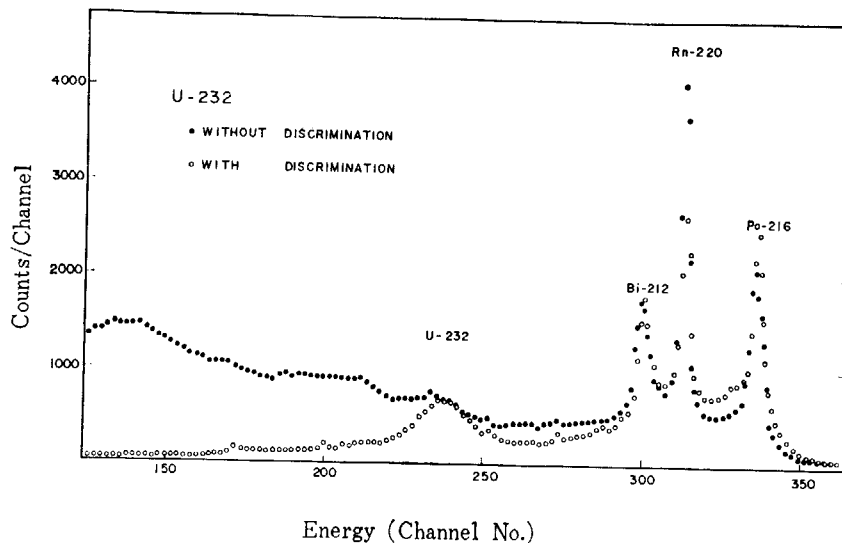


**Fig. 47** Beta-discrimination with a <sup>232</sup>U source.

show the effectiveness in this respect, a  $^{232}\text{U}$  source with an increased beta intensity was used; the  $^{232}\text{U}$  source was covered with a thin aluminum foil having an aperture, and the thickness of the foil was so chosen as to stop alphas but to be semi-transparent for the beta particles. By rise-time discrimination, the beta background was reduced considerably, and the  $^{232}\text{U}$  and  $^{228}\text{Th}$  (not indicated) peaks were clearly observed as seen in Fig. 47.

(2) Background from the surrounding materials (reduction of background neutrons)

The main causes for this background are radioactivities on the electrodes and chamber wall; another source is a gaseous substance such as  $^{220}\text{Rn}$  (thoron) in the present case of  $^{232}\text{U}$ . It is indicated theoretically that particles from the anode and the grid (towards the anode in the case from the grid) give rapid-rise pulses. These are shown in Fig. 48 as a peak of the rapid

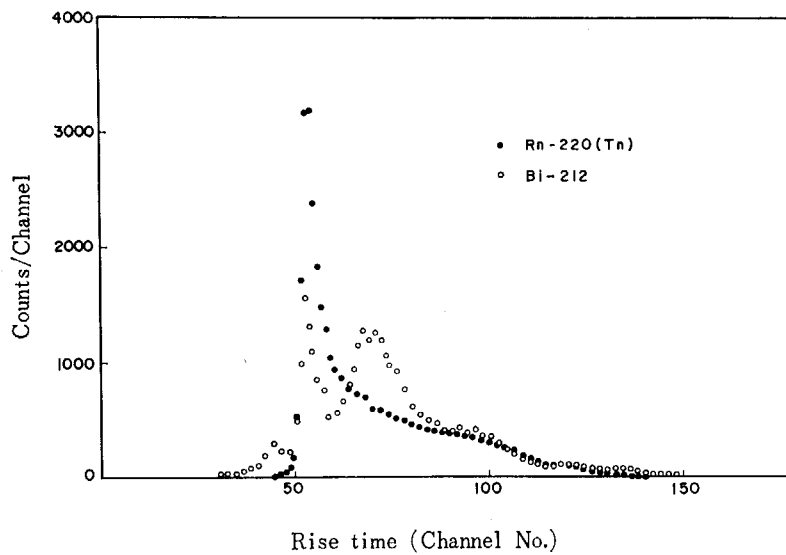


Fig. 48 Rise-time spectra of  $^{212}\text{Bi}$  and  $^{220}\text{Rn}(\text{Tn})$  alphas.

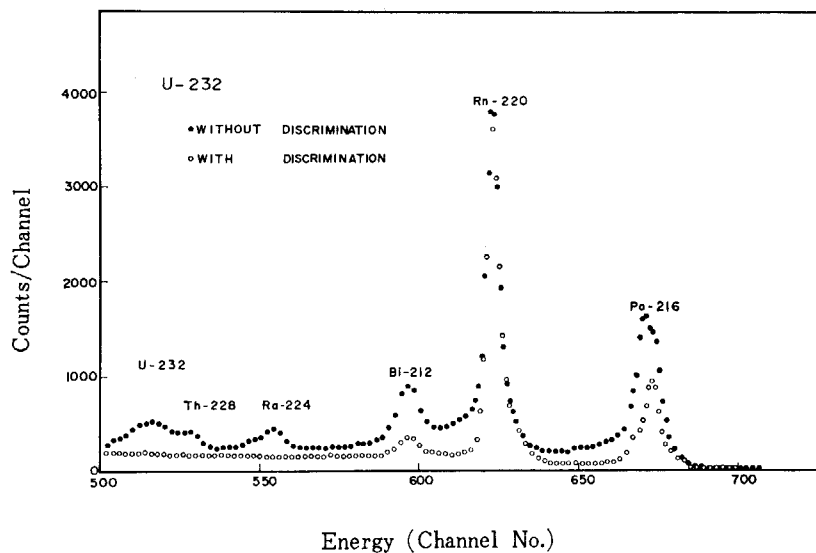


Fig. 49 Energy spectra for  $^{232}\text{U}$  source with and without rise-time discrimination. Only the  $^{220}\text{Rn}$  and daughters are observed for rapid-rise pulses.

rise-times in the rise-time spectrum of  $^{212}\text{Bi}$ . In this measurement,  $^{232}\text{U}$  was kept in the chamber for several days to deposit the daughter elements of thoron on the surrounding materials.

For thoron itself, however, no resolved peak was observed because the source was distributed throughout the chamber. Most of the thoron background was eliminated by the rise-

time discrimination as shown in Fig. 47.

To confirm these results, an alternative experiment was also performed. In this experiment, only the pulses with rapid rise-times were accepted and the peaks of thoron and the daughters alone were observed, as shown in Fig. 49.

### (3) Reduction of alpha background (reduction of large angle recoils)

When measuring alpha particles from a monoenergetic source, the spectrum is always with a continuum in the lower energy region. This is also observed even with a collimator. It is no problem in most cases, but gives trouble in the measurement of a weak activity together with an intense emitter of high energy. By the present method, the continuum is completely eliminated in a  $^{239}\text{Pu}$  spectrum, as shown in Fig. 50. This makes possible detection of weak

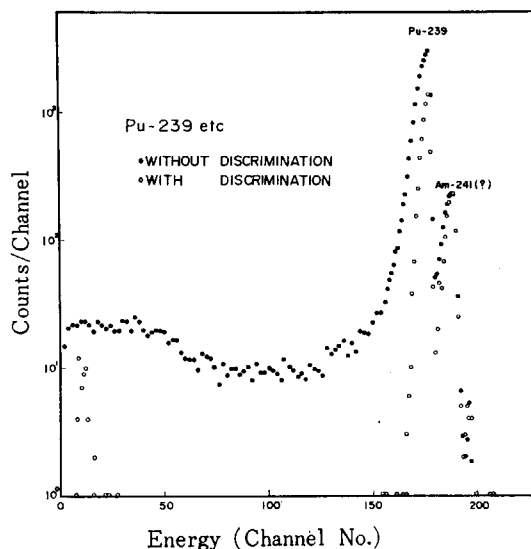


Fig. 50 Large angle rejection with a  $^{239}\text{Pu}$  source.

peaks in this region. The pulses in the extremely low energy region, close to the axis of ordinates as observed with rise-time discrimination, are caused by more penetrating particles.

It then should be noted that too strict discrimination will reject alpha particles of low energies. Fortunately, however, alpha particles from natural radionuclides have energies of 3 MeV~8 MeV, and there are no low-energy emitters below the region.

### (4) Improvement of energy resolution in a thick alpha source (particle collimation)

There are instances where the source was made thick from the counting statistics, and a thin source for the high energy resolution cannot be had. The method proposed is useful in such cases as this.

Degradation of the resolving power in a thick source is caused by two factors. One is the direction-dependent absorption in the source according to the angle  $\theta$ , and the other factor is the depth-dependent absorption for the given angle. The present method of electronic collimation eliminates the former contribution, which results in an improvement in the resolution, as shown in Fig. 51. In the figure, three peaks of  $^{232}\text{U}$ ,  $^{228}\text{Th}$  and  $^{224}\text{Ra}$  from a thick  $^{232}\text{U}$  source are shown for the different collimations; the closer the collimation, the better becomes the energy resolution. In Fig. 51, the collimation is defined as the "window" of the SCA for the fixed RHC setting.

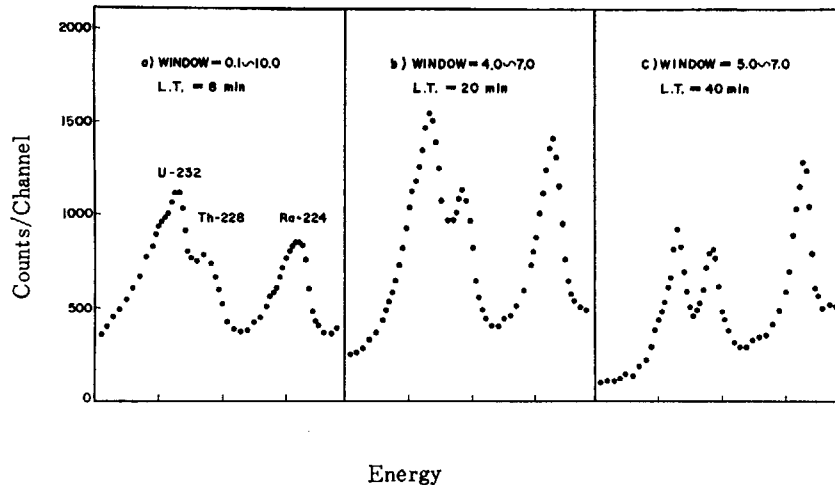


Fig. 51 Particle collimation with a  $^{232}\text{U}$  source.  
Energy resolution was improved by rise-time discrimination.

### (5) Conclusion

This method of rise-time discrimination also improves the quality of alpha spectra, in energy resolution, alpha continuum, beta background, and background arising from the surrounding materials.

The performance of the chamber was stable with 1 atm of P-10 gas as the working gas. For the energy information it was stable for a month or more, and for the rise-time information some instability observed in the first hour and disappeared subsequently.

There was some energy dependency of the collimation in the present method, as seen by comparison of the relative intensities of  $^{212}\text{Bi}$  and  $^{216}\text{Po}$  in Fig. 47. In a paper<sup>80)</sup> by other workers, it is indicated that the dependence is not significant. Fortunately, the alpha energies of most natural emitters are in a narrow range, *i. e.* from about 4 MeV to 7 MeV. On the other hand there is a possibility of reducing the dependency, by selecting quality of the rise-time information as described below.

Information of the rise-time can be varied by selecting the pick-off levels of RHC. From Fig. 43, it should be expected that the energy dependency of the information is nearly nullified by using a leading edge of  $t=0 \sim d/w_-$ . And the information of  $dE/dx$  may be obtained from the slope of the curve beyond  $t=d/w_-$ .

## 5. General Conclusion

Present methods of particle collimation, including a) with a multi-hole collimator, b) with fast coincidence technique in proportional counters, c) with rise-time discrimination in a proportional counter, d) with a combined method of the fast coincidence and rise-time methods, and e) with rise-time discrimination in a gridded ionization chamber, gave good results: A neutron spectrometer with a multi-hole collimator reduced the background due to chance coincidence by factor 5, and removed a summing problem of the outputs in the previous spectrometers. New methods referred as b), c) exhibited good performance for particle collimation and were used in a neutron spectrometer. Especially, the combined method d) improved the spectrum quality in a neutron spectrometry. A new method e) also proved a good collimating performance for alpha particles and showed a possibility of a new neutron spectrometer.

The rise-time discrimination in a proportional counter and a gridded ionization chamber was successfully used for the particle discrimination (neutron-gamma discrimination or alpha-beta discrimination).

The most notable improvement was a replacement of the collimator with an electronic collimation, which was made possible by the present methods. The background reduction, which is most important in a neutron spectrometry, will be achieved by these improvements.

The gas pressure must be adjusted to meet a given neutron energy. An alternative method is to use a counter gas of different stopping power: Pure hydrogen gas can be used for a lower energy region, and helium gas may be used for a higher region where He recoils are detected.

These spectrometers belong to the "differential" spectrum type. These are suitable to the detailed observation of a narrow energy region, though the "integral" type are suitable to obtain a general information over a wide range. The efficiency of "differential" spectrometers is not low compared with the "integral" spectrometers with a stripping method in which only the head-on information is utilized.

More detailed studies are necessary on the estimation of the spectrometer efficiency. Investigations on the insufficient volume or radial effect observed in the present method of collimation must also be performed for the efficiency estimation. A pulsed neutron technique combined with the computer technique will be useful in those studies.

## Acknowledgements

The author wants to acknowledge Mr. H. GOTOH, Mr. M. NOGUCHI, Mr. M. YAMADA, and Mr. S. TAKEGUCHI of the institute for valuable discussions and assistance. Thanks are also due to Mr. T. YAMANAKA and Mr. T. MIZOGUCHI, students of Tokyo Scientific University, for the assistance throughout the experiments. He is indebted to Dr. J. HIROTA and the gas counter group of FCA of the institute for the neutron-gamma discrimination in proportional counters.

He is also indebted to Dr. E. TERANISHI of Electrotechnical Laboratory, and to Mr. C. KOBAYASHI and Mr. S. KANDA of the institute for the experiments at the V. D. G. accelerators.

He would like to thank Professor T. SUITA of Osaka University and Mr. N. AMANO and Professor Y. MURAKAMI of the institute for the constant encouragement throughout the experiments, and Mr. K. MORI for the reading of the paper.

## References

- 1) BATCHELOR R., AVES R. and SKYRME T.H.R.: *Rev. Sci. Instr.* **26**, 1037 (1955)
- 2) OWEN R.B.: *I.R.E., NS-5*, 198 (1958)
- 3) AMALDI E., BOCCIARELLI D. and JRABACCHI G.: *Picerca Sci.* **12**, 830 (1941)
- 4) BARSCHALL H.H., ROSEN L., TASCHEK R.F. and WILLIAMS J.H.: *Revs. Modern Phys.* **24**, 1 (1952)
- 5) FOWLER J.L. and BROLLEY J.E.: *Revs. Modern Phys.* **28**, 103 (1956)
- 6) HILL D.L.: *Phys. Rev.* **87**, 1034 (1952)
- 7) WATT B.E.: *Phys. Rev.* **87**, 1037 (1952)
- 8) COCHRAN R.G. and HENRY K.M.: *Rev. Sci. Instr.* **26**, 757 (1955)
- 9) REID G.C.: *Proc. Phys. Soc. (London)* **A67**, 466 (1954)
- 10) HOLT J.R. and LITHERLAND A.E.: *Rev. Sci. Instr.* **25**, 298 (1954)
- 11) MOZLEY R.F. and SHOEMAKER F.C.: *Rev. Sci. Instr.* **23**, 569 (1952)
- 12) CALVERT J.M., JAFFE A.A. and MASLIN E.E.: *Proc. Phys. Soc. (London)* **A68**, 1017 (1955)
- 13) NEILER J.H., OWEN G.E., and ALLEN A.J.: *Phys. Rev.* **83**, 242 (A) (1951)
- 14) BEGHIAN L.E., ALLEN R.A., CALVERT J.M. and HALBAN H.: *Phys. Rev.* **86**, 1044 (1952)
- 15) DRAPER J.E.: *Rev. Sci. Instr.* **25**, 558 (1954)
- 16) GILES R.: *Rev. Sci. Instr.* **24**, 986 (1953)
- 17) BENENSON R.E. and SHURMAN M.B.: *Rev. Sci. Instr.* **29**, 1 (1958)
- 18) POOLE M.J.: *Proc. Phys. Soc. (London)* **A65**, 453 (1952)
- 19) ELIOT E.A., HICKS D., BEGHIAN L.E. and HALBAN H.: *Phys. Rev.* **94**, 144 (1954)
- 20) ZOLOTUKHIM V.G. et al.: *Atomnaya energiya*, **15**, 194 (1963)
- 21) VERBINSKI V.V., BURRUS W.R., FREESTONE R.M. and TEXTOR R.: ORNL-p-2471
- 22) SKYRME T.H.R., TUNNICLIFFE P.R. and WARD A.G.: *Rev. Sci. Instr.* **23**, 204 (1952)
- 23) BROEK H.W. and ANDERSON C.E.: *Rev. Sci. Instr.* **31**, 1063 (1960)
- 24) BATCHELOR R., GILBOY W.B., PARKER J.B. and TOWLE J.H.: *Nucl. Instr. Method.* **13**, 70 (1961)
- 25) WASSON M.M.: AERE-R4244
- 26) WASSON M.M.: AERE-R4269 (1963)
- 27) SWARTZ C.D., OWEN G.E. and AMES O.: AEC-NYO-2053
- 28) BENNET E.F.: *Rev. Sci. Instr.* **35**, 1153 (1962)  
: *Nucl. Sci. Engng.* **27**, 16 (1967)  
: ANL-6480 (1962)  
: ANL-6897 (1964)
- 29) BENJAMIN P.W., KEMSHALL C.D. and BRICKSTOCK A.: AWRE-O-9/68
- 30) BENJAMIN P.W., KEMSHALL C.D. and REDFEARN J.: AWRE-NR 1/64  
: AWRE-NR 2/64
- 31) WRIGHT G.T.: *Proc. Phys. Soc. (London)* **B69**, 358 (1956)
- 32) BROOKS F.D.: *Prg. Nucl. Phys.* **5**, 252 (1956)
- 33) OWEN R.B.: *I.R.E., NS-5*, 198 (1958)
- 34) FUNSTEN H.O. and COBB G.C.: *Rev. Sci. Instr.* **31**, 571 (1960)
- 35) FUSE T.: JAERI 1015
- 36) BATCHELOR R., GILBOY W.B., PURNELL A.D. and TOWLE J.H.: *Nucl. Instr. Method* **8**, 146 (1960)
- 37) HIRAMOTO T., NODA Y. and MIZUTANI T.: *Nucl. Instr. Method* **46**, 261 (1967)
- 38) DOKE T., ADACHI M., KUBOTA S. and Ogawa I.: *Nucl. Instr. Method* **57**, 163 (1967)
- 39) HIRAMOTO T. and NOHARA N.: *Nucl. Instr. Method* **58**, 167 (1968)
- 40) BROOKS F.D.: *Nucl. Instr. Method* **4**, 151 (1959)
- 41) BLOOM S.D., KAIFER R.C. and SCHRADER C.D.: *I.R.E., NS-7*, 170 (1960)
- 42) DAHEINICK W. and SHERR R.: *Rev. Sci. Instr.* **32**, 666 (1961)
- 43) OKANO K.: JAERI 1092
- 44) HAAS F.X. and MCCARTHY J.T.: *Nucl. Instr. Method* **50**, 340 (1967)



- 45) JOHNSON F. A. : *Nucl. Instr. Method* **58**, 134 (1968)
- 46) SABBABH B. and SUHAMI A. : *Nucl. Instr. Method* **58**, 102 (1968)
- 47) HOLLANDSWORTH C.E. and BUCHER W.P. : *Rev. Sci. Instr.* **39**, 165 (1968)
- 48) LARSEN R.N. : *Rev. Sci. Instr.* **37**, 514 (1966)
- 49) OBU M., ICHIMORI T., SHIRAKATA K., OGAWA H. and MIZUHO M. : JAERI-memo 3561 (1969)
- 50) DOBROZEMSKY R. and FELBER H. : ORNL-tr-1657
- 51) DOBROZEMSKY R. : "Development of an energy spectrometer for collimated neutrons of 50~300 keV".  
Diss., Univ. of Vinna, (1964)
- 52) MIZUHO M. : Japanese patent No. 530,333
- 53) SNIDOW N.L. and WARREN H.D. : *Nucl. Instr. Method* **51**, 109 (1967)
- 54) JOHNSON C.H. and TRAIL C.C. : *Rev. Sci. Instr.* **27**, 468 (1956)
- 55) GELLER K.N., ECCLESHALL D. and BARDIN T.T. : *Nucl. Instr. Method* **69**, 141 (1969)
- 56) JOHNSON C.H. : "Recoil telescope detectors" in *Fast Neutron Physics*, (J.B. MRION and J.L. FOWLER eds.; Interscience Publishers, Inc., London, (1960))
- 57) MIZUHO M. : German patent No. 1,244,764  
: U.S. patent No. 3,524,061  
: British patent No. 1,070,403  
: French patent No. 1,405,896  
: Japanese patent No. 474,535
- 58) PERLOW G.J. : *Rev. Sci. Instr.* **27**, 460 (1956)
- 59) LISKIEN H., NASTRI G. and PAULSEN A. : *Nucl. Instr. Method* **67**, 133 (1969)
- 60) CAPPELLANI F., CECCHI P.F. and FUBINI A. : EUR-2491. e
- 61) MIZUHO M. : Master thesis (Osaka University) (1960)
- 62) MIZUHO M. : *Nucl. Instr. Method* **75**, 85 (1969)
- 63) WHALING W. : in *Handbuch der Physik* **34** (FLUGGE S. ed.; Springer Verlag, Berlin, (1958)) p. 193.
- 64) BNL-325 (HUGHES D.J. and SCHWARTZ R.B. eds.; Brookhaven National Laboratory, Upton, New York, 1958) p.72
- 65) JAFFEY A.H. : *Rev. Sci. Instr.* **25**, 349 (1954)
- 66) MASKET A.V. : *Rev. Sci. Instr.* **28**, 191 (1957)
- 67) MIZUHO M. and YAMANAKA T. : *J. Nucl. Sci. Technol.* **7**, 285 (1970)
- 68) MIZUHO M. and MIZOGUCHI T. : *J. Nucl. Sci. Technol.* **7**, 335 (1970)
- 69) MIZUHO M. and YAMANAKA T. : *Nucl. Instr. Method.* **91**, 57 (1971)
- 70) SOYRES A. and Coppola M. : *Rev. Sci. Instr.* **35**, 431 (1964)
- 71) KUMAHARA T. : JAERI-memo 3605, 49 (1969)
- 72) KUMAHARA T. : JAERI-memo 2908, 32 (1967)
- 73) KINBARA S. : JAERI-memo 2908, 54 (1967)
- 74) KINBARA S. : JAERI-memo 3605, 33 (1969)  
: *Nucl. Instr. Method.* **70**, 173 (1969)
- 75) KOMAR A.P., VOROB'EV A.A. and KOROLYOV V.A. : *Dok. Akad. Nauk. SSSR.* **136**, 795 (1961)
- 76) VOROB'EV A.A., KOMAR A.P. and KOROLYOV V.A. : *Zh. Eksp. Teor. Fiz.* **43**, 426 (1962)
- 77) OGAWA I., DOKE T. and TSUKUDA M. : *Nucl. Instr. Method.* **13**, 169 (1961)
- 78) DOKE T. : *Canad. J. of Phys.* **40**, 607 (1962)
- 79) DOKE T., TSUKUDA M. and OGAWA I. : *J. Appl. Phys. Japan* **29**, 573 (1960)
- 80) FACCHINI U., GATTI E. and PELLEGRINI F. : *Nucl. Instr. Method.* **4**, 221 (1959)
- 81) MIZUHO M. and MIZOGUCHI T. : *Nucl. Instr. Method.* **91**, 439 (1971)
- 82) MIZUHO M. : *J. Nucl. Sci. Technol.* **7**, 476 (1970)
- 83) MIZUHO M. and NOGUCHI M. : *Nucl. Instr. Method.* **89**, 101 (1970)
- 84) ICHIMORI T., OBU M., SHIRAKATA K., OGAWA H. and MIZUHO M. : JAERI-memo 3580
- 85) MIZUHO M. : patent pend.
- 86) MIZUHO M. : patent pend.